World Academy of Science, Engineering and Technology
International Journal of Mechanical and Mechatronics Engineering
Vol:2, No:4, 2008

Controller Design for Euler-Bernoulli Smart Structures Using Robust Decentralized FOS via Reduced Order Modeling

T.C. Manjunath, *Student Member IEEE* , and B. Bandyopadhyay, *Member IEEE*

***Abstract*—**This paper features the modeling and design of a Robust Decentralized Fast Output Sampling (RDFOS) Feedback control technique for the active vibration control of a smart flexible multimodel Euler-Bernoulli cantilever beams for a multivariable (MIMO) case by retaining the first 6 vibratory modes. The beam structure is modeled in state space form using the concept of piezoelectric theory, the Euler-Bernoulli beam theory and the Finite Element Method (FEM) technique by dividing the beam into 4 finite elements and placing the piezoelectric sensor / actuator at two finite element locations (positions 2 and 4) as collocated pairs, i.e., as surface mounted sensor / actuator, thus giving rise to a multivariable model of the smart structure plant with two inputs and two outputs. Five such multivariable models are obtained by varying the dimensions (aspect ratios) of the aluminium beam. Using model order reduction technique, the reduced order model of the higher order system is obtained based on dominant Eigen value retention and the Davison technique. RDFOS feedback controllers are designed for the above 5 multivariable-multimodel plant. The closed loop responses with the RDFOS feedback gain and the magnitudes of the control input are obtained and the performance of the proposed multimodel smart structure system is evaluated for vibration control.

***Keywords*—**Smart structure, Euler-Bernoulli beam theory, Fast output sampling feedback control, Finite Element Method, State space model, Vibration control, LMI, Model order Reduction.

I. Introduction

PIEZOELECTRIC materials are capable of altering the structure's response through sensing, actuation and control. Piezoelectric elements can be incorporated into a laminated composite structure, either by embedding it or by mounting it onto the surface of the host structure [7]. Vibration control of any system is always a formidable challenge for any control system designer. Active control of vibrations relieves a designer from strengthening the structure from dynamic forces and the structure itself from extra weight and cost. The need for intelligent structures such as smart structures arises from the high performance requirements of such structural members in numerous applications. Intelligent structures are those which incorporate actuators and sensors that are highly integrated into the structure and have structural functionality, as well as highly integrated control logic, signal conditioning and power amplification electronics [3].

A vibration control system consists of 4 parts, viz., actuator, controller, sensor and the system or the plant, which is to be controlled. When an external force f_{ext} is applied to the beam, it is subjected to vibrations. These vibrations should be suppressed. Fully active actuators like the Piezoelectrics, MR Fluids, Piezoceramics, ER Fluids, Shape Memory Alloys, PVDF, etc., can be used to generate a secondary vibrational response in a mechanical system. This could reduce the overall response of the system plant by the destructive interference with the original response of the system, caused by the primary source of vibration [1], [6], [2], [5].

Extensive research in modeling of piezoelectric materials in building them as actuators and sensors for structures is reported in this paragraph. Investigations of Crawley and Luis [2] emphasized on the derivation of sensor / actuator modeling of piezo-electric materials. Moreover, the control analysis of cantilever beams using these sensors / actuators have been studied by Bailey and Hubbard [1]. Culshaw [3] gave a brief introduction to the concept of smart structure, its benefits and applications. Hanagud, *et al*., [6] developed a Finite Element Model (FEM) for an active beam with many distributed piezoceramic sensors / actuators coupled by signal conditioning systems and applied optimal output feedback control. Fanson *et.al.,* [5] performed some experiments on a beam with piezoelectrics using positive position feedback. Hwang and Park [7] presented a FE model for piezoelectric sensors and actuators. Feedback control of flexible structures was presented by Balas in [13]. Choi *et.al*. [4] discussed about the control techniques of flexible structures using distributed piezoelectric sensors / actuators. Feedback control of vibrations in mechanical systems has numerous applications, like in aircrafts, active noise and shape control, acoustic control, control of antennas, earthquake, structural health monitoring, control of space structures and in the control of flexible manipulators.

The outline of the paper is as follows. A brief review of related literature was given in the introductory section. Section 2 gives a brief introduction to the modeling technique

Mr. T. C. Manjunath is a Research Scholar in the Interdisciplinary Programme for Systems and Control Engineering, Indian Institute of Technology Bombay, Powai, Mumbai-400076, Maharashtra, India (Corresponding author phone : +91 22 25780263 / 25767884 ; fax: +91 22 25720057; e-mail: tcmanju@sc.iitb.ac.in, tcmanjunath@gmail.com, URL : http://www.sc.iitb.ac.in/~tcmanju).

Dr. B. Bandyopadhyay is with the Systems and Control Engineering of IIT Bombay, Mumbai-76, Maharashtra, India and is currently a Professor. (e-mail : bijnan@ee.iitb.ac.in, URL : http://www.sc.iitb.ac.in/~bijnan).

(sensor / actuator model, finite element model, state space model) of the smart flexible cantilever beam for a multivariable case with two inputs and two outputs. A brief review of the controlling technique, viz., the fast output sampling feedback control technique, multimodel synthesis, design of the LMI formulation, model order reduction technique and the design of the robust decentralized fast output sampling feedback controller to control the first six modes of vibration of the system via the reduced order modeling is discussed in section 3. The controller design is presented in section 4. Conclusions are drawn in section 5 followed by the simulation results.

II. Mathematical Modeling of Smart Beam

Consider a flexible cantilever beam made of aluminum bonded with piezoelectric sensor / actuator all along the length of the beam as shown in Fig. 1. The dimensions and properties of the flexible beam and piezoelectric sensor / actuator are given in Tables 1 and 2 respectively.

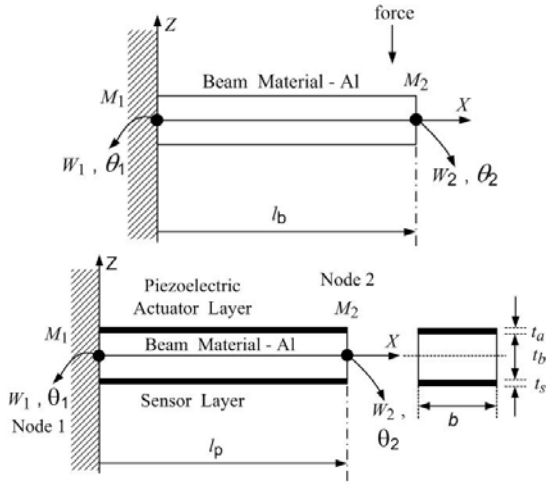

Fig. 1 A regular flexible beam and a smart flexible beam. F_1 and F_2 : Forces at node 1 and 2, M_1 and M_2 : Moments at node 1 and 2, l_b : Length of beam , l_p : Length of piezo-layer

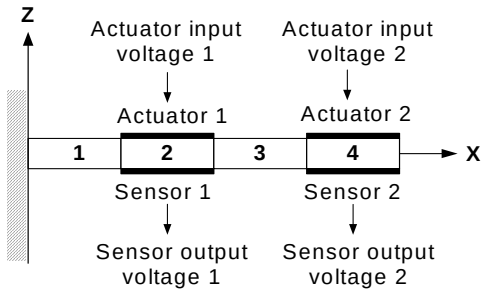

Fig. 2 A smart flexible beam divided into 4 finite elements with piezo patches placed at even FE positions 2 and 4

The flexible cantilever beam as shown in Fig. 1 is divided into a number of finite elements viz., 4 as shown in Fig. 2. The piezoelectric sensor / actuator is bonded to the master structure at finite element positions numbering 2 and 4, thus giving rise to a Multiple Input Multiple Output (MIMO) system with 2 actuator inputs u_1, u_2 to the actuators and 2 sensor outputs, y_1, y_2 from the sensors.

TABLE I
Physical Parameters
Properties of the Flexible Cantilever Beam Element

Parameter (with units)	Symbol	Numerical values
Total length (m)	l_b	0.5
Width (m)	b	0.024
Young's modulus (GPa)	E_b	193.06
Density (kg / m^3)	ρ_b	8030
Constants used in $\mathbf{C}^*$	α, β	0.001. 0.0001
Thickness	t_b	Varying from 0.5 mm to 1 mm, i.e., to give 5 models

TABLE II
Properties of the (PZT) Piezo - Sensor / Actuator

Parameter (with units)	Symbol	Numerical values
Length (m)	l_p	0.125
Width (m)	b	0.024
Thickness (mm)	t_a, t_s	0.5
Young's modulus (GPa)	E_p	68
Density (kg / m^3)	ρ_p	7700
Piezoelectric stress constant (VmN^{-1})	g_{31}	10.5×10^{-13}
Piezo strain constant (m / V)	d_{31}	125×10^{-12}

A. Modeling of Regular and Piezo Elements of Beam

To start with, we consider the modeling of the regular beam element and the piezoelectric beam element as shown in the Fig. 1. The dynamic model for the smart structure is developed using the Finite Element Method (FEM) [7], [15]. The smart cantilever beam model is developed using a piezoelectric beam element, which includes the sensor and actuator dynamics and a regular beam element based on Euler-Bernoulli theory assumptions. The piezoelectric beam element is used to model the regions where the piezoelectric element is bonded as sensor / actuator and the rest of the structure is modeled by the regular beam elements.

In modeling and analysis of the smart beam, the following assumptions are made. The perfect bonding or the adhesive between the beam and the sensor / actuator and the thin film electrode surfaces have been assumed to add no mass or stiffness to the sensor / actuator, i.e., neglected. The cable capacitance between sensor and signal-conditioning device has been considered negligible and the temperature effects have been neglected. The signal conditioning device gain (G_c) is assumed as 100. The free vibration characteristics of a flexible beam is governed by the following fourth order differential equation [21], [22]

$$c^2 \frac{\partial^4 w(x,t)}{\partial x^4} + \frac{\partial^2 w(x,t)}{\partial t^2} = 0, \quad (1)$$

where w is the transverse displacement of the beam and is a function x and t, x being the distance of the local coordinate from the fixed end, t being the time and c is a constant which is given by $\sqrt{EI/\rho A}$.

E, I, ρ and A are the young's modulus, moment of inertia, mass density and area of the beam respectively. When a system vibrates, it undergoes to and fro motion and so all positions vary with time and therefore, the system has velocities and accelerations. Mass times acceleration as inertia force appears in the governing differential equation of the beam which is given in Eq. (1), i.e., the equation of motion involves a fourth order derivative w.r.t. x and a second order derivative w.r.t. time.

The piezoelectric element is obtained by sandwiching the regular beam element between two thin piezoelectric layers as shown in Fig. 2. The bottom layer is acting as a sensor and the top layer acts as an actuator. The beam element is assumed to have two structural DOF (w, θ) at each nodal point and an electrical DOF: a transverse deflection and an angle of rotation or slope. Since the voltage is constant over the electrode, the number of electrical DOF is one for each element.

The electrical DOF is used as a sensor voltage or actuator voltage when the piezoelectric material attached to the structure behaves as sensor or actuator. Corresponding to the 2 DOF, a transverse shear force and a bending moment acts at each nodal point. At each nodal point, counteracting moments induced by the piezoelectric actuators will be acting. The bending moment resulting from the applied voltage to the actuator adds a positive finite element being the moment at node 1 while subtracting it at node 2.

The deflection behavior of the beam element is best described by a displacement function $W(x)$, which is the solution of Eq. (1). It is desirable that this function satisfies the differential equation of equilibrium for the beam element. The solution of the Eq. (1) is assumed as a cubic polynomial function of x given by [21], [22]

$$W(x) = a_1 + a_2 x + a_3 x^2 + a_4 x^3, \quad (2)$$

where the constants a_1 to a_4 are obtained using the boundary conditions of the beam at the nodal points (fixed end and free end) as

$$\begin{bmatrix} a_1 \\ a_2 \\ a_3 \\ a_4 \end{bmatrix} = \frac{1}{l_b^3} \begin{bmatrix} l_b^3 & 0 & 0 & 0 \\ 0 & l_b^3 & 0 & 0 \\ -3l_b & -2l_b^2 & 3l_b & -l_b^2 \\ 2 & l_b & -2 & l_b \end{bmatrix} \begin{bmatrix} w_1 \\ \theta_1 \\ w_2 \\ \theta_2 \end{bmatrix}. \quad (3)$$

where w_1, θ_1 and w_2, θ_2 are the DOF's at the node 1 (fixed end) and node 2 (free end) respectively.

The Eq. (2) is rearranged in the final form as

$$[W(x)] = [\mathbf{n}^T][\mathbf{q}], \quad (4)$$

where $[\mathbf{n}^T]$ gives the shape functions of the beam $f_i(x),\ i = 1,..,4$ as

$$[\mathbf{n}^T] = \begin{bmatrix} f_1(x) & f_2(x) & f_3(x) & f_4(x) \end{bmatrix}, \quad (5)$$

where

$$\mathbf{n} = \begin{bmatrix} 1 - 3\frac{x^2}{l_b^2} + 2\frac{x^3}{l_b^3} \\ x - 2\frac{x^2}{l_b} + \frac{x^3}{l_b^2} \\ 3\frac{x^2}{l_b^2} - 2\frac{x^3}{l_b^3} \\ -\frac{x^2}{l_b} + \frac{x^3}{l_b^2} \end{bmatrix}, \quad (6)$$

where x is the local axial coordinate of the finite element node from the fixed end, l_b being the length of the beam and $\mathbf{q}$ is the vector of displacements and slopes (nodal displacement vector) and is given by

$$\mathbf{q} = \begin{bmatrix} w_1 \\ \theta_1 \\ w_2 \\ \theta_2 \end{bmatrix} \quad (7)$$

for the beam shown in Fig. 1. The displacement, its first, second spatial derivatives and its time derivative in matrix form is given by $W(x)$, $W'(x)$, $W''(x)$ and $\dot{W}(t)$ as

$$[W'(x)] = [\mathbf{n}_2^T][\mathbf{q}],$$

$$\frac{\partial W}{\partial x} = \begin{bmatrix} f_1'(x) & f_2'(x) & f_3'(x) & f_4'(x) \end{bmatrix} \begin{bmatrix} w_1 \\ \theta_1 \\ w_2 \\ \theta_2 \end{bmatrix}, \quad (8)$$

$$[W''(x)] = [\mathbf{n}_1^T][\mathbf{q}],$$

$$\frac{\partial^2 W}{\partial x^2} = \begin{bmatrix} f_1''(x) & f_2''(x) & f_3''(x) & f_4''(x) \end{bmatrix} \begin{bmatrix} w_1 \\ \theta_1 \\ w_2 \\ \theta_2 \end{bmatrix}, \quad (9)$$

$$[\dot{W}(x)] = [\mathbf{n}_3^T][\dot{\mathbf{q}}];$$

$$\frac{\partial W(x)}{\partial t} = \begin{bmatrix} f_1(x) & f_2(x) & f_3(x) & f_4(x) \end{bmatrix} \begin{bmatrix} \dot{w}_1 \\ \dot{\theta}_1 \\ \dot{w}_2 \\ \dot{\theta}_2 \end{bmatrix}. \quad (10)$$

B. Piezoelectric Strain Rate Sensors and Actuators

The linear piezoelectric coupling [12] between the elastic field and the electric field is expressed by the direct and the converse piezoelectric equations as

$$D = d\,T + \varepsilon^T E, \quad S = s^E T + d\,E, \quad (11)$$

where T is the stress, S is the strain, E is the electric field, D

is the dielectric displacement, ε is the permittivity of the medium, s^E is the compliance of the medium and d is the piezoelectric constant .

C. Sensor Equation

The direct piezoelectric equation is used to calculate the output charge created by the strain in the structure [12]. Since no external field is applied to the sensor layer, the electric displacement developed on the sensor surface is directly proportional to the strain acting on the sensor. If the poling is done along the thickness direction of the sensors with the electrodes on the upper and lower surfaces, the electric displacement is given as

$$D_z = d_{31} * E_p \varepsilon_x = e_{31} \varepsilon_x , \tag{12}$$

where e_{31} is the piezoelectric stress / charge constant, E_p is the Young's modulus and ε_x is the strain of the testing structure at a point on the beam.

The total charge $Q(t)$ developed on the sensor surface is the spatial summation of all the point charges developed on the sensor layer. Since the current $i(t) = \frac{d\ Q(t)}{dt}$ suggests that the closed-circuit current signal generated in a piezoelectric lamina is proportional to the strain rate of the testing structure, we obtain

$$i(t) = z\, e_{31}\, b \int_0^{l_p} \mathbf{n}_1^T \dot{\mathbf{q}}\, dx , \tag{13}$$

where $z = \frac{t_b}{2} + t_a$, b is the width of the beam, l_p being the length of the piezo-sensor and $\mathbf{n}_1^T$ is the second spatial derivative of shape function of the flexible beam. This current is converted into the open circuit sensor voltage V^s using a signal-conditioning device with the gain G_c and applied to the actuator with the controller gain K_c. The sensor output voltage is obtained as

$$V^s(t) = G_c\, e_{31}\, z\, b \int_0^{l_p} \mathbf{n}_1^T \dot{\mathbf{q}}\, dx , \tag{14}$$

which is nothing but the signal conditioning gain G_c multiplied by the closed circuit current $i(t)$ generated by the piezoelectric lamina. Substituting for $\mathbf{n}_1^T$ from Eq. (8) and $\dot{\mathbf{q}}$ from Eq. (10) and simplifying, we get the sensor voltage for a two node finite element of the beam as

$$V^s(t) = \begin{bmatrix} 0 & -G_c\, e_{31}\, z\, b & 0 & G_c\, e_{31}\, z\, b \end{bmatrix} \begin{bmatrix} \dot{w}_1 \\ \dot{\theta}_1 \\ \dot{w}_2 \\ \dot{\theta}_2 \end{bmatrix}$$

$$= G_c\, e_{31}\, z\, b * \begin{bmatrix} 0 & -1 & 0 & 1 \end{bmatrix} \begin{bmatrix} \dot{w}_1 \\ \dot{\theta}_1 \\ \dot{w}_2 \\ \dot{\theta}_2 \end{bmatrix} , \tag{15}$$

which can be further expressed as a scalar-vector product

$$V^s(t) = \mathbf{p}^T \dot{\mathbf{q}} , \tag{16}$$

where $\dot{\mathbf{q}}$ is the time derivative of the modal coordinate vector $\mathbf{q}$, $\mathbf{p}^T$ is a constant vector which depends on the type of sensor, its characteristics and its location on the beam. Note that the sensor output is a function of the second spatial derivative of the mode shape. This sensor voltage is given as input to the controller and the output of the controller (which is nothing but the control input to the actuator, i.e., the actuator voltage) is the controller gain K_c multiplied by the sensor voltage $V^s(t)$. Thus, the input voltage to the actuator $V^a(t)$ is given by

$$V^a(t) = K_c\ V^s(t) . \tag{17}$$

Substituting for $V^s(t)$ from Eq. (14) in Eq. (17), we get

$$V^a(t) = K_c\, G_c\, e_{31}\, z\, b \int_0^{l_p} \mathbf{n}_1^T \dot{\mathbf{q}}\, dx . \tag{18}$$

D. Actuator Equation

The actuator strain is derived from the converse piezoelectric equation. The strain developed ε_a on the actuator layer is given by [12]

$$\varepsilon_a = d_{31} E_f , \tag{19}$$

where d_{31} and E_f are the piezo strain constant and the electric field respectively. When the input to the piezoelectric actuator $V^a(t)$ is applied in the thickness direction t_a, the electric field, E_f which is the voltage applied $V^a(t)$ divided by the thickness of the actuator t_a; and the stress, σ_a which is the actuator strain multiplied by the young's modulus E_p of the piezo actuator layer are given by

$$E_f = \frac{V^a(t)}{t_a} \tag{20}$$

and

$$\sigma_a = E_p\, d_{31} \frac{V^a(t)}{t_a} . \tag{21}$$

The resultant moment M_A acting on the beam is determined by integrating the stress throughout the structure thickness as

$$M_A = E_p\, d_{31}\, \bar{z}\ V^a(t) , \tag{22}$$

where $\bar{z} = \frac{(t_a + t_b)}{2}$, is the distance between the neutral axis of the beam and the piezoelectric layer. The moment results

in the generation of the control force. Finally, the control force applied by the actuator is obtained as

$$f_{ctrl} = E_p\, d_{31}\, b\, \bar{z} \int_{l_p} \mathbf{n}_2\, dx\, V^a(t) \tag{23}$$

or can be expressed as a scalar vector product as

$$f_{ctrl} = \mathbf{h}\, V^a(t) = \mathbf{h}\, u(t)\ , \tag{24}$$

where $\mathbf{n}_2{}^T$ is the first spatial derivative of the shape function of the flexible beam, $\mathbf{h}^T$ is a constant vector which depends on the type of actuator and its location on the beam, given by $\mathbf{h} = \begin{bmatrix} -E_p\, d_{31}\, b\, \bar{z} & 0 & E_p\, d_{31}\, b\, \bar{z} & 0 \end{bmatrix}$ and $u(t)$ is nothing but the control input to the actuator, i.e., $V^a(t)$ from the controller. If any external forces described by the vector $\mathbf{f}_{ext}$ are acting on the beam, then the total force vector becomes

$$f^t = f_{ext} + f_{ctrl}\ . \tag{25}$$

E. Dynamic Equation of Smart Structure

The strain energy U and the kinetic energy T for the beam element with uniform cross section in bending is [21], [22]

$$U = \frac{E_b\, I_b}{2} \int_{l_b} \left[\frac{\partial^2 w}{\partial x^2} \right]^2 dx = \frac{E_b\, I_b}{2} \int_{l_b} \left[w''(x,t) \right]^T \left[w''(x,t) \right] dx\ , \tag{26}$$

$$T = \frac{\rho_b\, A_b}{2} \int_{l_b} \left[\dot{w}(x,t) \right]^2 dx\ = \frac{\rho_b\, A_b}{2} \int_{l_b} \left[\dot{w}(x,t) \right]^T \left[\dot{w}(x,t) \right] dx\ . \tag{27}$$

The equation of motion of the regular beam element is obtained by the Lagrangian equation for the regular beam element as

$$\frac{d}{dt} \left[\frac{\partial T}{\partial \dot{q}_i} \right] + \left[\frac{\partial U}{\partial q_i} \right] = \left[F_i \right], \tag{28}$$

which after simplification yields as

$$M^b\, \ddot{q} + K^b\, q = f^b(t)\ , \tag{29}$$

where

$$\left[M^b \right] = \rho_b A_b \int_{l_b} \left[\mathbf{n}_3 \right]^T \left[\mathbf{n}_3 \right] dx\ , \tag{30}$$

$$\left[M_{ij}{}^b \right] = \rho_b A_b \int_{l_b} f_i(x)\, f_j(x)\, dx \tag{31}$$

and

$$\left[K^b \right] = E_b I_b \int_{l_b} \left[\mathbf{n}_1 \right]^T \left[\mathbf{n}_1 \right] dx\ , \tag{32}$$

$$\left[K_{ij}{}^b \right] = E_b I_b \int_{l_b} f_i''(x)\, f_j''(x)\, dx\ . \tag{33}$$

Finally, after simplification, we get

$$M^b = \frac{\rho_b A_b l_b}{420} \begin{bmatrix} 156 & 22 l_b & 54 & -13 l_b \\ 22 l_b & 4 l_b{}^2 & 13 l_b & -3 l_b{}^2 \\ 54 & 13 l_b & 156 & -22 l_b \\ -13 l_b & -3 l_b{}^2 & -22 l_b & 4 l_b{}^2 \end{bmatrix} \tag{34}$$

and

$$K^b = \frac{E_b I_b}{l_b} \begin{bmatrix} 12/l_b{}^2 & 6/l_b & -12/l_b{}^2 & 6/l_b \\ 6/l_b & 4 & -6/l_b & 2 \\ -12/l_b{}^2 & -6/l_b & 12/l_b{}^2 & -6/l_b \\ 6/l_b & 2 & -6/l_b & 4 \end{bmatrix}, \tag{35}$$

where M^b, K^b are the local mass matrix, the local stiffness matrix of the regular beam element.

Similarly, the lagrangian equation of motion for the piezoelectric beam element is obtained as

$$M^p\, \ddot{q} + K^p\, q = f^p(t), \tag{36}$$

where M^p and K^p are the piezoelectric beam element mass matrix and stiffness matrix and are given as

$$M^p = \frac{\rho A l_p}{420} \begin{bmatrix} 156 & 22 l_p & 54 & -13 l_p \\ 22 l_p & 4 l_p{}^2 & 13 l_p & -3 l_p{}^2 \\ 54 & 13 l_p & 156 & -22 l_p \\ -13 l_p & -3 l_p{}^2 & -22 l_p & 4 l_p{}^2 \end{bmatrix}, \tag{37}$$

$$K^p = \frac{E I}{l_p} \begin{bmatrix} 12/l_p{}^2 & 6/l_p & -12/l_p{}^2 & 6/l_p \\ 6/l_p & 4 & -6/l_p & 2 \\ -12/l_p{}^2 & -6/l_p & 12/l_p{}^2 & -6/l_p \\ 6/l_p & 2 & -6/l_p & 4 \end{bmatrix}, \tag{38}$$

where

$$EI = E_b I_b + 2 E_p I_p\ , \tag{39}$$

$$I_p = \frac{1}{12} b t_a{}^3 + b t_a \left(\frac{t_a + t_b}{2} \right)^2\ , \tag{40}$$

and

$$\rho A = b \left(\rho_b\, t_b + 2\, \rho_p\, t_a \right). \tag{41}$$

The dynamic equation of the smart structure is obtained by using both the regular and piezoelectric beam elements given by Eqs. (29) and (36). The mass and stiffness of the bonding or the adhesive between the master structure and the sensor / actuator pair is neglected. The mass and stiffness of the entire beam, which is divided into 4 finite elements is assembled using the FEM technique [7], [15] and the assembled matrices (global matrices), $\mathbf{M}$ and $\mathbf{K}$ are obtained. The equation of motion of the smart structure is finally given by

$$\mathbf{M}\, \ddot{\mathbf{q}} + \mathbf{K}\mathbf{q} = f_{ext} + f_{ctrl} = f^t\ , \tag{42}$$

where $\mathbf{M}$, $\mathbf{K}$, $\mathbf{q}$, f_{ext}, f_{ctrl}, f^t are the global mass matrix, global stiffness matrix of the smart beam, the vector of displacements and slopes, the external force applied to the beam, the controlling force from the actuator and the total force coefficient vector respectively. The mass matrix $\mathbf{M}$, stiffness matrix $\mathbf{K}$ and the control force vector $\mathbf{h}^T$ in the system equation can be varied by changing the position and number of regular and piezoelectric beam elements.

The generalized coordinates are introduced into the Eq. (42) using a transformation $\mathbf{q} = \mathbf{T}\mathbf{g}$ in order to reduce it further

such that the resultant equation represents the dynamics of the first 6 vibratory modes ω_1 to ω_6 of the smart flexible cantilever beam. $\mathbf{T}$ is the modal matrix containing the eigen vectors representing the first 6 vibratory modes. This method is used to derive the uncoupled equations governing the motion of the free vibrations of the system in terms of principal coordinates by introducing a linear transformation between the generalized coordinates $\mathbf{q}$ and the principal coordinates $\mathbf{g}$. The Eq. (42) now becomes

$$\mathbf{M}\,\mathbf{T}\ddot{\mathbf{g}} + \mathbf{K}\,\mathbf{T}\mathbf{g} = f_{ext} + f_{ctrl\,1} + f_{ctrl\,2}, \tag{43}$$

where $f_{ctrl\,1}$ and $f_{ctrl\ 2}$ are the control force coefficient vectors to the actuators from the controller.

Multiplying Eq. (43) by $\mathbf{T}^T$ on both sides and further simplifying, we get

$$\mathbf{M}^*\ddot{\mathbf{g}} + \mathbf{K}^*\mathbf{g} = \mathbf{f}^*_{ext} + \mathbf{f}^*_{ctrl\,1} + \mathbf{f}^*_{ctrl\,2}, \tag{44}$$

where $\mathbf{M}^* = \mathbf{T}^T\mathbf{M}\mathbf{T}$, $\mathbf{K}^* = \mathbf{T}^T\mathbf{K}\mathbf{T}$, $\mathbf{f}^*_{ext} = \mathbf{T}^T\mathbf{f}_{ext}$, $\mathbf{f}^*_{ctrl\,i} = \mathbf{T}^T\mathbf{f}_{ctrl\,i}$ $i = 1$ to 2.

$\mathbf{M}^*$, $\mathbf{K}^*$, $\mathbf{f}^*_{ext}$, $\mathbf{f}^*_{ctrl\,1}$, $\mathbf{f}^*_{ctrl\,2}$ represents the generalized mass matrix, the generalized stiffness matrix, the generalized external force vector and the generalized control force vectors respectively.

The generalized structural modal damping matrix $\mathbf{C}^*$ (Raleigh proportional damping) is introduced into the Eq. (44) by using

$$\mathbf{C}^* = \alpha\,\mathbf{M}^* + \beta\,\mathbf{K}^*, \tag{45}$$

where α and β are the structural damping constants respectively.

The dynamic equation of the smart flexible cantilever beam developed is obtained as

$$\mathbf{M}^*\ddot{\mathbf{g}} + \mathbf{C}^*\dot{\mathbf{g}} + \mathbf{K}^*\mathbf{g} = \mathbf{f}^*_{ext} + \mathbf{f}^*_{ctrl}, \tag{46}$$

where $\mathbf{f}^*_{ctrl} = \mathbf{f}^*_{ctrl\,1} + \mathbf{f}^*_{ctrl\,2}$.

F. State Space Model of the Smart Structure

The state space model of the smart flexible cantilever beam is obtained as follows [21], [22]. Let

$$\mathbf{g} = \begin{bmatrix} x_1 \\ x_2 \\ \vdots \\ x_6 \end{bmatrix} \text{ and } \dot{\mathbf{g}} = \begin{bmatrix} x_7 \\ x_8 \\ \vdots \\ x_{12} \end{bmatrix}. \tag{47}$$

$$\therefore, \dot{\mathbf{g}} = \begin{bmatrix} \dot{x}_1 \\ \dot{x}_2 \\ \vdots \\ \dot{x}_6 \end{bmatrix} = \begin{bmatrix} x_7 \\ x_8 \\ \vdots \\ x_{12} \end{bmatrix} \text{ and } \ddot{\mathbf{g}} = \begin{bmatrix} \dot{x}_7 \\ \dot{x}_8 \\ \vdots \\ \dot{x}_{12} \end{bmatrix}. \tag{48}$$

Thus,

$$\begin{aligned} &\dot{x}_1 = x_7\ ,\ \dot{x}_2 = x_8\ ,\ \dot{x}_3 = x_9\ , \\ &\dot{x}_4 = x_{10}\ ,\ \dot{x}_5 = x_{11}\ ,\ \dot{x}_6 = x_{12} \end{aligned} \tag{49}$$

and Eq. (46) now becomes

$$\mathbf{M}^*\begin{bmatrix} \dot{x}_7 \\ \dot{x}_8 \\ \dot{x}_9 \\ \dot{x}_{10} \\ \dot{x}_{11} \\ \dot{x}_{12} \end{bmatrix} + \mathbf{C}^*\begin{bmatrix} x_7 \\ x_8 \\ x_9 \\ x_{10} \\ x_{11} \\ x_{12} \end{bmatrix} + \mathbf{K}^*\begin{bmatrix} x_1 \\ x_2 \\ x_3 \\ x_4 \\ x_5 \\ x_6 \end{bmatrix} = \mathbf{f}^*_{ext} + \mathbf{f}^*_{ctrl}, \tag{50}$$

which can be further simplified as

$$\begin{bmatrix} \dot{x}_7 \\ \dot{x}_8 \\ \dot{x}_9 \\ \dot{x}_{10} \\ \dot{x}_{11} \\ \dot{x}_{12} \end{bmatrix} = -\mathbf{M}^{*-1}\mathbf{K}^*\begin{bmatrix} x_1 \\ x_2 \\ x_3 \\ x_4 \\ x_5 \\ x_6 \end{bmatrix} - \mathbf{M}^{*-1}\mathbf{C}^*\begin{bmatrix} x_7 \\ x_8 \\ x_9 \\ x_{10} \\ x_{11} \\ x_{12} \end{bmatrix} + \mathbf{M}^{*-1}\mathbf{f}^*_{ext} + \mathbf{M}^{*-1}\mathbf{f}^*_{ctrl}. \tag{51}$$

The generalized external force coefficient vector is

$$\mathbf{f}^*_{ext} = \mathbf{T}^T f_{ext} = \mathbf{T}^T f\, r(t), \tag{52}$$

where $r(t)$ is the external force input (impulse disturbance) to the beam.

The generalized control force coefficient vector is

$$\mathbf{f}^*_{ctrl\,i} = \mathbf{T}^T f_{ctrl\,i} = \mathbf{T}^T\mathbf{h}_i V_i^a(t) = \mathbf{T}^T\mathbf{h}_i u_i(t), \quad i = 1 \text{ to } 2, \tag{53}$$

where the voltages $V_i^a(t)$ are the input voltages to the actuators 1 and 2 from the controllers respectively, and are nothing but the control inputs $u_i(t)$ to the actuators, $\mathbf{h}_i$ is a constant vector which depends on the actuator type, its position on the beam and is given by

$$\begin{aligned} \mathbf{h}_1 &= E_p\, d_{31}\, b\, \bar{z}\, \begin{bmatrix} -1 & 1 & \ldots\ldots 0 & 0 \end{bmatrix}_{8\times 1} \\ &= a_c \begin{bmatrix} -1 & 1 & \ldots\ldots 0 & 0 \end{bmatrix} \end{aligned} \tag{54}$$

for one piezoelectric actuator element (say, for the piezo patch placed at the finite element position numbering 2), where $E_p\, d_{31}\, b\, \bar{z} = a_c$ being the actuator constant. So, using the Eqs. (52) and (53) in Eq. (51), the state space equation for the smart beam is represented as

$$\begin{bmatrix} \dot{x}_1 \\ \dot{x}_2 \\ \vdots \\ \dot{x}_{12} \end{bmatrix} = \begin{bmatrix} 0 & I \\ -\mathbf{M}^{*-1}\mathbf{K}^* & -\mathbf{M}^{*-1}\mathbf{C}^* \end{bmatrix}_{(12\times 12)} \begin{bmatrix} x_1 \\ x_2 \\ \vdots \\ x_{12} \end{bmatrix}_{(12\times 1)} +$$

$$\begin{bmatrix} 0 & 0 \\ \mathbf{M}^{*-1}\mathbf{T}^T\mathbf{h}_1 & \mathbf{M}^{*-1}\mathbf{T}^T\mathbf{h}_2 \end{bmatrix}_{(12\times 2)} \begin{bmatrix} u_1 \\ u_2 \end{bmatrix}_{(2\times 1)} + \begin{bmatrix} 0 \\ \mathbf{M}^{*-1}\mathbf{T}^T f \end{bmatrix}_{(12\times 1)} r(t), \quad (55)$$

i.e., $$\dot{\mathbf{X}} = \mathbf{A}\,x(t) + \mathbf{B}\,u(t) + \mathbf{E}\,r(t). \quad (56)$$

The sensor voltage is taken as the output of the system and its equation is modeled as

$$V_i^s(t) = \mathbf{p}_i^T \dot{\mathbf{q}} = y_i(t),\ i=1,2, \quad (57)$$

where $\mathbf{p}_i^T$ is a constant vector which depends on the piezoelectric sensor characteristics (i.e., the sensor constant S_c) and on the position of the sensor location on the beam. The constant vector for the sensor placed at finite element position numbering 4 is given by

$$\begin{aligned} \mathbf{p}_2^T &= G_c\, e_{31}\, z\, b \begin{bmatrix} 0 & 0 & \ldots\ldots & -1 & 1 \end{bmatrix}_{1\times 8} \\ &= S_c \begin{bmatrix} 0 & 0 & \ldots\ldots & -1 & 1 \end{bmatrix}, \end{aligned} \quad (58)$$

where $G_c\, e_{31}\, z\, b = S_c$ is the sensor constant.

Thus, the sensor output is given by

$$y(t) = \mathbf{p}^T \dot{\mathbf{q}} = \mathbf{p}^T\,\mathbf{T}\dot{\mathbf{g}} = \mathbf{p}^T\,\mathbf{T} \begin{bmatrix} x_1 \\ x_2 \\ x_3 \\ x_4 \\ x_5 \\ x_6 \end{bmatrix}, \quad (59)$$

which can be written as

$$\begin{bmatrix} y_1 \\ y_2 \end{bmatrix} = \begin{bmatrix} 0 & \mathbf{p}_1^T \\ 0 & \mathbf{p}_2^T \end{bmatrix}_{(2\times 12)} \begin{bmatrix} x_1 \\ x_2 \\ \vdots \\ x_{12} \end{bmatrix}_{(12\times 1)} \quad (60)$$

for a multivariable case with 2 inputs and 2 outputs. i.e.,

$$y(t) = \mathbf{C}^T\,x(t) + \mathbf{D}\,u(t). \quad (61)$$

The multivariable state space model (state equation and the output equation) of the smart structure developed for the system thus [21], [22], is given by

$$\begin{aligned} \dot{\mathbf{x}} &= \mathbf{A}\,x(t) + \mathbf{B}\,u(t) + \mathbf{E}\,r(t), \\ y(t) &= \mathbf{C}^T\,x(t) + \mathbf{D}\,u(t), \end{aligned} \quad (62)$$

with

$$\mathbf{A} = \begin{bmatrix} 0 & I \\ -\mathbf{M}^{*-1}\mathbf{K}^* & -\mathbf{M}^{*-1}\mathbf{C}^* \end{bmatrix}_{(12\times 12)},$$

$$\mathbf{B} = \begin{bmatrix} 0 & I \\ \mathbf{M}^{*-1}\mathbf{T}^T\mathbf{h}_1 & \mathbf{M}^{*-1}\mathbf{T}^T\mathbf{h}_2 \end{bmatrix}_{(12\times 2)}, \quad (63)$$

$$C^T = \begin{bmatrix} 0 & \mathbf{p}_1^T \\ 0 & \mathbf{p}_2^T \end{bmatrix}_{(2\times 12)},\ \mathbf{D} = \text{a null matrix},$$

$$\mathbf{E} = \begin{bmatrix} 0 \\ \mathbf{M}^{*-1}\mathbf{T}^T\mathbf{f} \end{bmatrix}_{(12\times 1)},$$

where $r(t), u(t), \mathbf{A}, \mathbf{B}, \mathbf{C}, \mathbf{D}, \mathbf{E}, x(t)$ and $y(t)$ represents the external force input, the control input, system matrix, input matrix, output matrix, transmission matrix, external load matrix, state vector, system output (sensor output).

By considering the thickness of the beam in the model 1 as 0.5 mm, thickness of the beam in model 2 as 0.6 mm, thickness of the beam in model 3 as 0.7 mm, thickness of the beam in the model 4 as 0.8 mm and thickness of the beam in the model 5 as 1 mm, 5 multivariable state space models (multi-model) of the same smart structure plant are obtained as shown in Eq. (62).

These 5 MIMO models give rise to a multimodel smart structure plant. Let $(\mathbf{A}_i, \mathbf{B}_i, \mathbf{C}_i, \mathbf{D}_i, \mathbf{E}_i)$; $i=1,2,3,4,5$ be the state space matrices of the 5 models of the beam. State space model of the smart cantilever beam with sensor / actuator pair at element 2 and 4 for the model 1 for 6 modes is represented by Eq. (62) with

$$\mathbf{C}_1^T = \begin{bmatrix} 0 & 0 & 0 & 0 & 0 & 0 & -0.0404 & -0.0453 \\ 0 & 0 & 0 & 0 & 0 & 0 & 0.2084 & -0.1783 \\ 0.0415 & -0.0044 & -0.0212 & -0.0200 \\ -0.1050 & 0.0455 & 0.1427 & -0.1254 \end{bmatrix},$$

$$\mathbf{B}_1 = \begin{bmatrix} 0 & 0 \\ 0 & 0 \\ 0 & 0 \\ 0 & 0 \\ 0 & 0 \\ 0 & 0 \\ 16.5924 & -21.3687 \\ -7.1011 & 25.4467 \\ 13.5529 & 15.3619 \\ -6.5758 & 9.1164 \\ -0.4503 & 3.9458 \\ -0.3630 & -0.4057 \end{bmatrix};\ \mathbf{E}_1 = 10^3 \begin{bmatrix} 0 \\ 0 \\ 0 \\ 0 \\ 0 \\ 0 \\ -2.4449 \\ 1.6580 \\ 0.7635 \\ 0.4944 \\ 0.3082 \\ -0.1110 \end{bmatrix}, \quad (64)$$

$$\mathbf{D}_1 = \text{Null matrix},$$

$$\mathbf{A}_1 = 10^6 * \begin{bmatrix} 0 & 0 & 0 & 0 & 0 & 0 \\ 0 & 0 & 0 & 0 & 0 & 0 \\ 0 & 0 & 0 & 0 & 0 & 0 \\ 0 & 0 & 0 & 0 & 0 & 0 \\ 0 & 0 & 0 & 0 & 0 & 0 \\ 0 & 0 & 0 & 0 & 0 & 0 \\ -2.992 & 0.0 & -0.0 & -0.0 & -0.0 & 0.0 \\ -0.0 & -1.082 & 0.0 & 0.0 & -0.0 & -0.0 \\ -0.0 & -0.0 & -0.2836 & -0.0 & 0.0 & -0.0 \\ 0.0 & 0.0 & -0.0 & -0.0661 & 0.0 & 0.0 \\ -0.0 & -0.0 & -0.0 & -0.0 & -0.0080 & 0.0 \\ -0.0 & -0.0 & 0.0 & -0.0 & 0.0 & -0.0001 \end{bmatrix}$$

$$\begin{bmatrix} 0 & 0 & 0 & 0 & 0 & 0 \\ 0 & 0 & 0 & 0 & 0 & 0 \\ 0 & 0 & 0 & 0 & 0 & 0 \\ 0 & 0 & 0 & 0 & 0 & 0 \\ 0 & 0 & 0 & 0 & 0 & 0 \\ 0 & 0 & 0 & 0 & 0 & 0 \\ -0.0004 & 0.0 & -0.0 & -0.0 & -0.0 & 0.0 \\ -0.0 & -0.0002 & 0.0 & 0.0 & -0.0 & -0.0 \\ -0.0 & -0.0 & -0.0 & -0.0 & 0.0 & -0.0 \\ 0.0 & 0.0 & -0.0 & -0.0 & 0.0 & 0.0 \\ -0.0 & -0.0 & -0.0 & -0.0 & -0.0 & 0.0 \\ -0.0 & -0.0 & 0.0 & -0.0 & 0.0 & -0.0 \end{bmatrix}$$

The state space models of the remaining 4 models are obtained similarly. The characteristics of the smart flexible cantilever beam of the model 1 are given in Table III.

TABLE III
CHARACTERISTICS OF THE SMART FLEXIBLE BEAM FOR THE MULTIVARIABLE MODEL 1

Models	EIGEN VALUES	Natural Frequency (Hz.)
Model 1	$-0.0071 \pm j\ 9.36$	1.4892
	$-0.5975 \pm j\ 89.2$	14.1995
	$-4.96 \pm j\ 257.1$	40.9239
	$-21.3 \pm j\ 532.1$	84.6910
	$-81.2 \pm j\ 1037.2$	165.0721
	$-224.4 \pm j\ 1715.1$	272.9711

Similarly, the characteristics of the other 4 models are obtained.

III. DESIGN OF CONTROLLER VIA THE REDUCED ORDER MODELING

In the following section, we develop the control strategy for the multivariable cum multimodel representation of the developed smart structure model using the fast output sampling feedback control law [9], [10], [14] with 1 actuator input u and 1 sensor output y for the 5 models of the smart structure plant as shown in Fig. 2. In this type of control law as shown in Fig. 3, the value of the input at a particular moment depends on the output value at a time prior to this moment (namely at the beginning of the period). Werner and Furuta [14], Chammas and Leondes [16] have shown that the poles of the discrete time control system could be assigned arbitrarily (within the natural restriction that they should be located symmetrically with respect to the real axis) using the fast output sampling technique. Since the feedback gains are piecewise constants, their method could easily be implemented, guarantees the closed loop stability and indicated a new possibility. Such a control law can stabilize a much larger class of systems.

A. Fast Output Sampling

Consider a plant described by a LTI state space model given by

$$\dot{x}(t) = A\,x(t) + B\,u(t), \quad y(t) = C\,x(t), \tag{65}$$

where $x \in \Re^n$, $u \in \Re^m$, $y \in \Re^p$, $A \in \Re^{n\times n}$, $B \in \Re^{n\times m}$, $C \in \Re^{p\times n}$, A, B, C, are constant matrices of appropriate dimensions and it is assumed that the model is controllable and observable. Assume that output measurements are available at time instants $t = k\tau$, where $k = 0, 1, 2, 3, \ldots$. Now, construct a discrete linear time invariant system from these output measurements at sampling rate $\frac{1}{\tau}$ (sampling interval of τ secs) during which the control signal u is held constant. The system obtained so is called as the τ system and is given by

$$\begin{aligned} x((k+1)\tau) &= \Phi_\tau\, x(k\tau) + \Gamma_\tau\, u(k\tau), \\ y(k\tau) &= C\,x(k\tau), \end{aligned} \tag{66}$$

where $\Phi_\tau, \Gamma_\tau, C$ are constant matrices of appropriate dimensions. Assume that the plant is to be controlled by a digital computer, with sampling interval τ and zero order hold and that a sampled data state feedback design has been carried out to find a state feedback gain F such that the closed loop system

$$x(k\tau + \tau) = (\Phi_\tau + \Gamma_\tau F)x(k\tau) \tag{67}$$

has desirable properties.

Let $\Delta = \frac{\tau}{N}$, where $N >$ the observability index υ of the system. The control signal $u(k)$, which is applied during the interval $k\tau \le t \le (k+1)\tau$ is then generated according to

$$\begin{aligned} u(k) &= \begin{bmatrix} L_0 & L_1 & \ldots\ldots & L_{N-1} \end{bmatrix} \begin{bmatrix} y(k\tau - \tau) \\ y(k\tau - \tau + \Delta) \\ : \\ : \\ y(k\tau - \Delta) \end{bmatrix}, \\ &= L\,y_k \end{aligned} \tag{68}$$

where the matrix blocks L_j represent the output feedback gains and the notation L, y_k has been introduced here for convenience. Note that $\frac{1}{\tau}$ is the rate at which the loop is closed, whereas the output samples are taken at the times N-times faster rate $\frac{1}{\Delta}$. To show how a FOS controller in Eqn. (68) can be designed to realize the given sampled data state feedback gain for a controllable and observable system, we construct a fictitious, lifted system for which the Eqn. (68) can be interpreted as static output feedback [8], [16]. Let (Φ, Γ, C) denote the system in Eqn. (65) sampled at the rate $\frac{1}{\Delta}$. Consider the discrete time system having at time $t = k\tau$, the input $u_k = u(k\tau)$, the state $x_k = x(k\tau)$ and the output y_k as

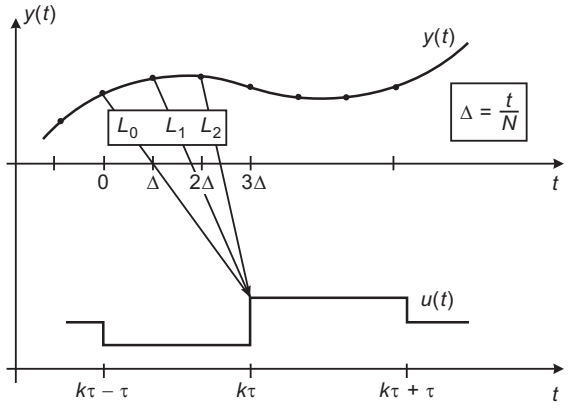

Fig. 3 Graphical illustration of fast output sampling feedback method

$$x_{k+1} = \Phi_\tau x_k + \Gamma_\tau u_k, \quad y_{k+1} = \mathbf{C}_0 x_k + \mathbf{D}_0 u_k, \tag{69}$$

where

$$\mathbf{C}_0 = \begin{bmatrix} C \\ C\Phi \\ \vdots \\ C\Phi^{N-1} \end{bmatrix}; \ \mathbf{D}_0 = \begin{bmatrix} 0 \\ C\Gamma \\ \vdots \\ C\sum_{j=0}^{N-2} \Phi^j \Gamma \end{bmatrix}. \tag{70}$$

Now, design a state feedback gain F such that $(\Phi_\tau + \Gamma_\tau F)$ has no Eigen values at the origin and provides the desired closed loop behavior. Then, assuming that in the interval $k\tau \le t \le (k\tau + \tau)$,

$$u(t) = F\, x(k\tau), \tag{71}$$

one can define the fictitious measurement matrix,

$$\mathbf{C}(F, N) = (\mathbf{C}_0 + \mathbf{D}_0 F)(\Phi_\tau + \Gamma_\tau F)^{-1}, \tag{72}$$

which satisfies the fictitious measurement equation

$$y_k = \mathbf{C}\, x_k. \tag{73}$$

For L to realize the effect of F, it must satisfy the equation.

$$\mathbf{LC} = F. \tag{74}$$

Let υ denote the observability index of (Φ, Γ, C). It can be shown that for $N \ge \upsilon$, generically $\mathbf{C}$ has full column rank, so that any state feedback gain can be realized by a fast output sampling gain $\mathbf{L}$. If the initial state is unknown, there will be an error $\Delta u_k = u_k - F\, x_k$ in constructing the control signal under the state feedback; one can verify that the closed-loop dynamics are governed by

$$\begin{bmatrix} x_{k+1} \\ \Delta u_{k+1} \end{bmatrix} = \begin{bmatrix} \Phi_\tau + \Gamma_\tau F & \Gamma_\tau \\ 0 & \mathbf{LD}_0 - F\Gamma_\tau \end{bmatrix} \begin{bmatrix} x_k \\ \Delta u_k \end{bmatrix}. \tag{75}$$

The system in Eqn. (69) is stable if F stabilizes and only if (Φ_τ, Γ_τ) and the matrix $(\mathbf{LD}_0 - F\Gamma_\tau)$ has all its Eigen values inside the unit circle. It is evident that the eigen values of the closed loop system under a FOS control law are those of $(\Phi_\tau + \Gamma_\tau F)$ together with those of $(\mathbf{LD}_0 - F\Gamma_\tau)$. This suggests that the state feedback F should be obtained so as to ensure the stability of both $(\Phi_\tau + \Gamma_\tau F)$ and $(\mathbf{LD}_0 - F\Gamma_\tau)$.

The problem with controllers obtained in this way is that, although they are stabilizing and achieve the desired closed loop behavior in the output sampling instants, they may cause an excessive oscillation between sampling instants. The fast output sampling feedback gains obtained may be very high. To reduce this effect, we relax the condition that $\mathbf{L}$ exactly satisfy the linear equation (74) and include a constraint on the gain $\mathbf{L}$. Thus, we arrive at the following in Eqn. (76) as

$$\begin{aligned} &\|\mathbf{L}\| < \rho_1, \\ &\|\mathbf{LD}_0 - F\Gamma_\tau\| < \rho_2, \\ &\|\mathbf{LC} - F\| < \rho_3, \end{aligned} \tag{76}$$

where ρ_1, ρ_2 and ρ_3 represents the upper bounds on the spectral norms of $\mathbf{L}$, $(\mathbf{LD}_0 - F\Gamma_\tau)$ and $(\mathbf{LC} - F)$. This can be formulated in the form of Linear Matrix Inequalities as

$$\begin{aligned} &\begin{bmatrix} -\rho_1^2 I & \mathbf{L} \\ \mathbf{L}^T & -I \end{bmatrix} < 0, \\ &\begin{bmatrix} -\rho_2^2 I & \mathbf{LD}_0 - F\Gamma_\tau \\ (\mathbf{LD}_0 - F\Gamma_\tau)^T & -I \end{bmatrix} < 0, . \\ &\begin{bmatrix} -\rho_3^2 I & \mathbf{L}C - F \\ (\mathbf{L}C - F)^T & -I \end{bmatrix} < 0. \end{aligned} \tag{77}$$

In this form, the LMI control optimization toolbox is used for the synthesis of $\mathbf{L}$ [11]. Here, ρ_1 means low noise

sensitivity, ρ_2 small means fast decay of observation error, and most importantly, ρ_3 small means that the FOS controller with gain $\mathbf{L}$ is a good approximation of the originally designed state feedback controller. If $\rho_3 = 0$, then $\mathbf{L}$ is an exact solution.

If suitable bounds ρ_1, ρ_2 are known, one can keep these bounds fixed and minimize ρ_3 under these constraints. This requires a search for a FOS controller which gives the best approximation of the given state feedback designed under the constraints represented by ρ_1 and ρ_2. It should be noted here that closed loop stability requires $\rho_2 < 1$, i.e., the eigen values which determine the error dynamics must lie within the unit disc. In this form, the function mincx ( ) of the LMI control toolbox for MATLAB can be used to minimize a linear combination of ρ_1, ρ_2 and ρ_3.

B. Multimodel Synthesis

One feature of the fast output sampling control that makes it attractive for robust controller design is the fact that a result similar to the above can be shown to hold when the same state feedback is applied simultaneously to a family of plant models representing different operating conditions of the plant. For multimodel representation of a plant, it is necessary to design controller, which will robustly stabilize the multimodel system. Multimodel representation of the plants can arise in several ways. When a non-linear system has to be stabilized at different operating points, linear models are sought to be obtained at those operating points. Even for parametric uncertain linear systems, different linear models can be obtained for extreme points of the parameters. These models are used for the stabilization of the uncertain systems. Now, instead of a single model, consider a family of plant models (A_i, B_i, C_i) defined by

$$\dot{x} = A_i x + B_i u, y = C_i x \;;\; i = 1, 2, 3, 4, \ldots\ldots M. \quad (78)$$

By sampling at the rate of $1/\Delta$, we get a family of discrete time systems (Φ_i, Γ_i, C_i). Now, consider the augmented system defined as

$$\widetilde{\Phi} = diag(\Phi_1 \ldots\ldots\ldots \Phi_M) = \begin{bmatrix} \Phi_1 & 0 & \ldots\ldots & 0 \\ 0 & \Phi_2 & \ldots\ldots & \vdots \\ \vdots & \vdots & \ddots & \vdots \\ 0 & 0 & \ldots\ldots & \Phi_M \end{bmatrix}, \quad (79)$$

$$\widetilde{\Gamma} = diag(\Gamma_1 \ldots\ldots\ldots \Gamma_M) = \begin{bmatrix} \Gamma_1 & 0 & \ldots\ldots & 0 \\ 0 & \Gamma_2 & \ldots\ldots & \vdots \\ \vdots & \vdots & \ddots & \vdots \\ 0 & 0 & \ldots\ldots & \Gamma_M \end{bmatrix}, \quad (80)$$

$$\widetilde{C} = \begin{bmatrix} C_1 & C_2 & \ldots\ldots & C_M \end{bmatrix}, i = 1 \text{ to } M, \text{ where } M = 5. \quad (81)$$

Consider the family of discrete time systems obtained from Eqn. (82) having at time $t = k\tau$, the input $u_k = u(k\tau)$, the state vector $x_k = x(k\tau)$ and output y_k as

$$x_{k+1} = \Phi_{\tau i} x_k + \Gamma_{\tau i} u_k, \quad y_{k+1} = \mathbf{C}_{0i} x_k + \mathbf{D}_{0i} u_k, \quad (82)$$

where

$$\mathbf{C}_{0i} = \begin{bmatrix} C_i \\ C_i \Phi_i \\ \vdots \\ C_i \Phi_i^{N-1} \end{bmatrix}, \mathbf{D}_0 = \begin{bmatrix} 0 \\ C_i \Gamma_i \\ \vdots \\ C_i \sum_{j=0}^{N-2} \Phi_i{}^j \Gamma_i \end{bmatrix}. \quad (83)$$

Assume that $(\Phi_{\tau i}, \Gamma_i)$ are controllable. Then, we can find robust state feedbacks gain F such that $(\Phi_{\tau i} + \Gamma_{\tau i} F)$ has no eigen values at the origin and the system responses has a good settling time. Then, assuming that in the interval $k\tau \le t \le (k\tau + \tau)$,

$$u(t) = F x(k\tau), \quad (84)$$

one can define the fictitious measurement matrix,

$$\mathbf{C}_i(F, N) = (\mathbf{C}_{0i} + \mathbf{D}_{0i} F)(\Phi_{\tau i} + \Gamma_{\tau i} F)^{-1}, \quad (85)$$

which satisfies the fictitious measurement equation

$$y_k = \mathbf{C}_i x_k. \quad (86)$$

For robust fast output sampling gain L to realize the effect of F, it may satisfy

$$\mathbf{L}\mathbf{C}_i = F, \; i = 1 \text{ to } M, i.e., 5. \quad (87)$$

The Eqn. (87) can be written as

$$\mathbf{L}\widetilde{\mathbf{C}} = \widetilde{F}, \quad (88)$$

where

$$\widetilde{\mathbf{C}} = \begin{bmatrix} C_1 & C_2 & C_3 & C_4 & C_5 \end{bmatrix} \quad (89)$$

are the new fictitious output measurement matrices for the individual plant models and

$$\widetilde{F} = \begin{bmatrix} F_1, F_2, F_3, F_4, F_5 \end{bmatrix}. \quad (90)$$

With a fast output sampling gain which satisfies Eqn. (88), for each model the closed loop eigen values are those of

$$\begin{bmatrix} \Phi_{\tau i} + \Gamma_{\tau i} F & \Gamma_{\tau i} \\ 0 & \mathbf{L}\mathbf{D}_{0i} - F_i \Gamma_{\tau i} \end{bmatrix}, \quad i = 1, \ldots, 5. \quad (91)$$

which shows that the closed loop eigen values are still the ones for which the state feedback gains F_i have been designed, together with those of $\mathbf{L}\mathbf{D}_{0i} - F_i \Gamma_{\tau i}$.

C. An LMI formulation of the design problem for a robust FOS feedback controller

Let $\widetilde{\upsilon}$ denote the observability index of $(\widetilde{\Phi}, \widetilde{\Gamma}, \widetilde{C})$. It can be shown that for $N \ge \widetilde{\upsilon}$, generically $\widetilde{\mathbf{C}}$ has full column rank, so that the robust state feedback gain can be realized by

a fast output sampling gain $\mathbf{L}$. When this idea is realized in practice, i.e., fast output sampling gain $\mathbf{L}$ have been obtained by realizing the state feedback gain F , two problems are required to be addressed.

The first one is apparent from Eqn. (75). The fact that the closed loop eigen values are the eigen values of Eqn. (91) means that the closed loop plant dynamics can be designed without considering the dynamics of the observation error which are determined by the eigen values of $\left(\mathbf{LD}_{0i} - F_i\Gamma_{\tau i}\right)$. On the other hand, the choice of F_i constrains the design of the latter.

With this type of controller, the unknown states are estimated implicitly, using the measured output samples and assuming that the initial control is generated by state feedback. If the initial state causes an estimation error, then decay of this error will be determined by the eigen values of the matrix $\left(\mathbf{LD}_{0i} - F_i\Gamma_{\tau i}\right)$ which depends on $\mathbf{L}$ and whose dimension equals the number of control inputs. For stability, these eigen values have to be inside the unit disc and for fast decay they should be as close to the origin as possible. This problem must be taken into account while designing $\mathbf{L}$.

The second problem is that the gain matrix $\mathbf{L}$ may have elements with large magnitude because of noise sensitivity. Because, these values are only weights in linear combination of output samples, large magnitudes do not necessarily imply large control signal and in control theory and in noise free simulation problem, they pose no problem.

But, in practice, they amplify measurement noise and it is desirable to keep these values low. It is feasible to improve the performance by not insisting that $\mathbf{LC}_i = F$ is satisfied exactly, but a slight deviation can be allowed which in turn yields smaller gains. The following method allows a design of $\mathbf{L}$ such that the spectral norm of $\mathbf{LD}_{0i} - F\Gamma_{\tau i}$ and hence $\mathbf{L}$ as well as the distance between $\mathbf{LC}$ and F can be controlled. This objective can be expressed by an upper bound ρ on the norm of the gain matrix $\mathbf{L}$ as follows.

While trying to deal with these problem, it is better not to insist on an exact solution to the design of Eqn. (87), one can allow a small deviation and use an approximation $\mathbf{LC}_i \approx F$, which hardly affects the desired closed loop dynamics, but may have considerable effect on the two problems described above. Instead of looking for an exact solution to the equalities, the following inequalities are solved.

$$\begin{gathered} \left\|\mathbf{L}\right\| < \rho_1, \\ \left\|\mathbf{LD}_{0i} - F\Gamma_{\tau i}\right\| < \rho_{2i}\,,\ i = 1,...,5\,, \\ \left\|\mathbf{LC}_i = F\right\| < \rho_{3i}\,. \end{gathered} \tag{92}$$

ρ_1, ρ_2, ρ_3 represent the upper bounds on the spectral norms of $\mathbf{L}$, $\mathbf{LD}_0 - F\Gamma_\tau$ and $\mathbf{LC} - F$ respectively. These 3 objectives have been expressed by the upper bounds on matrix norms and each should be as small as possible. ρ_1 means low noise sensitivity, ρ_2 small means fast decay of observation error and most importantly, ρ_3 small means that fast output sampling controller with gain $\mathbf{L}$ is a good approximation of the originally designed state feedback controller. If $\rho_3 = 0$, then $\mathbf{L}$ is an exact solution. Using the schur compliment, it is straight forward to bring these conditions in the form of LMI's as follows.

$$\begin{gathered} \begin{bmatrix} -\rho_{1i}{}^2 I & \mathbf{L} \\ \mathbf{L}^T & -I \end{bmatrix} < 0\,, \\ \begin{bmatrix} -\rho_{2i}{}^2 I & \mathbf{LD}_{0i} - F\Gamma_{\tau i} \\ \left(\mathbf{LD}_{0i} - F\Gamma_{\tau i}\right)^T & -I \end{bmatrix} < 0 \\ \begin{bmatrix} -\rho_{3i}{}^2 I & \mathbf{LC}_i - F \\ \left(\mathbf{LC}_i - F\right)^T & -I \end{bmatrix} < 0 \end{gathered} \tag{93}$$

In this form, the function mincx ( ) of the LMI control tool box for Matlab can be used immediately to minimize a linear combination of ρ_1, ρ_2, ρ_3 . The following approach turned out to be useful. If the actual measurement noise is known, the magnitude of $\mathbf{L}$ is fixed accordingly. Likewise the eigen values of $\left(\mathbf{LD}_{\tau i} - F\Gamma_{\tau i}\right) < 0.05$ cause no problem. So, we fix ρ_1, ρ_2 and only ρ_3 is minimized subject to these constraints.

This requires a search for a fast output sampling controller, which gives the best approximation of the given state feedback, designed under the constraints represented by ρ_1, ρ_2 . It should be noted here that closed loop stability requires $\rho_2 < 1$, i.e., the eigen values which determine the error dynamics must like within the unit disc. In this form, the LMI tool box of Matlab can be used for synthesis [11]. The fast output sampling feedback controller obtained by the above method requires only constant gains and hence is easier to implement.

D. Model Order Reduction Technique

For many complex processes or when the modes of a dynamical system are very high, the order of the state matrix may be quite large. It would be difficult to work with these large scale dynamical systems [19] in their original form. In such cases, it is common to study the process by approximating it to a simpler model. These mathematical models correspond to approximating a system by its dominant pole-zeros in the complex plane. They generally require empirical determination of the system parameters. Many different methods have been developed to accomplish the purpose by estimating the 'dominant' part of the large system

and finding a simpler (or reduced order) system representation that has its behaviour akin to the original system.

Here, we discuss the model order reduction technique based on the dominant modes retention. It is usually possible to describe the dynamics of a physical dynamical system by a number of simultaneous linear differential equations with constant coefficients as

$$\dot{x} = Ax + Bu,\ \ y = Cx, \tag{94}$$

where A is a $(n \times n)$ matrix.

The simulation and design of controllers become very cumbersome if the order of the system goes high. One way to overcome this difficulty is to develop a reduced model of the higher order system. One of the well known technique is based on dominant eigenvalue retention based on the Davison technique [17], [18]. By this method, a system of higher order can be numerically approximated to one of smaller order. The method suggests that a large $(n \times n)$ system can be reduced to a simpler $(r \times r)$ model $(r \le n)$by considering the effects of the r most dominant (dominant in the sense of being closest to the instability) eigenvalues alone.

The principle of the method is to neglect the eigen values of the original system that are farthest from the origin and retain only the dominant eigenvalues and hence dominant time constants of the original system in the reduced order model. This implies that the overall behaviour of the approximate system will be very similar to that of the original system since the contribution of the unretained eigenvalues to the system response are important only at the beginning of the response, whereas the eigenvalues retained are important throughout the whole of the response. For the system represented by the Eqn. (94), consider the linear transformation,

$$x = P z, \tag{95}$$

which transforms the model Eqn. (94) into the following form,

$$\dot{z} = \hat{A} z + \hat{B} u,\ \ y = \hat{C} z, \tag{96}$$

where $\hat{A}$ is a $(r \times r)$ matrix and

$$\hat{A} = P^{-1} A P,\ \hat{B} = P^{-1} B \text{ and } \hat{C} = C P. \tag{97}$$

$\hat{A}$ is in the diagonal form as

$$\hat{A} = diag\left[\lambda_1, \lambda_2, ..., \lambda_n\right] \tag{98}$$

and

$$Re(\lambda_1) \ge Re(\lambda_2) \ge ..... \ge Re(\lambda_n). \tag{99}$$

Further, assume that only r eigenvalues are dominant, i.e., the order of the reduced model is r and partition the model in Eqn. (96) as

$$\dot{z}_1 = \hat{A}_1 z_1 + \hat{B}_1 u,\ \dot{z}_2 = \hat{A}_2 z_2 + \hat{B}_2 u$$

and

$$y = \hat{C}_1 z_1 + \hat{C}_2 z_2 \tag{100}$$

where

$$\begin{aligned} \hat{A}_1 &= diag\left[\lambda_1, \lambda_2, ..., \lambda_r\right], \\ \hat{A}_2 &= diag\left[\lambda_{r+1}, \lambda_{r+2}, ..., \lambda_n\right], \\ \hat{B}_1 &= \text{first } r \text{ rows of } \hat{B},\ \hat{B}_2 \\ &= \text{remaining}\,(n-r) \text{ rows of } \hat{B} \end{aligned} \tag{101}$$

and are respectively $(r \times r)$, $(n-r) \times (n-r)$, $(r \times m)$ and $(n-r) \times m$ matrices obtained by portioning of $\hat{A}$ and $\hat{B}$ suitably. In Eqn. (100), the order of z_1 is r and that of z_2 is $(n-r)$. Now, because the contribution of the modes represented by the eigenvalues $\lambda_{r+1}, \lambda_{r+2}, ..., \lambda_n$ is not significant, it may be assumed that $z_2 = 0$, whereby we have from Eqn. (95),

$$\begin{bmatrix} x_1 \\ x_2 \end{bmatrix} = \begin{bmatrix} P_{11} \\ P_{21} \end{bmatrix} z_1, \tag{102}$$

where P_{11} and P_{21} are respectively, $(r \times r)$ and $(n-r) \times r$ submatrices obtained by portioning of P_1 and z_1, z_2 are respectively, r and $(n-r)$ dimensional state vectors corresponding to the original state variables. It follows from Eqn. (102) that

$$z_1 = P_{11}^{-1} x_1, \tag{103}$$

with which the model in Eqn. (100) can be transformed to

$$\dot{x}_1 = P_{11} \hat{A}_1 P_{11}^{-1} x_1 + P_{11} \hat{B} u = A_x x_1 + B_r u$$

and

$$y = \hat{C}_1 P_{11}^{-1} x_1 = C_r x_1 \tag{104}$$

Moreover, from Eqns. (102), and (103), we have

$$x_2 = P_{21} P_{11}^{-1} x_1. \tag{105}$$

Thus, the original n^{th} order model represented by Eqn. (94) is reduced to an r^{th} order model given by Eqn. (104). The state variables of the approximate model are the same as the first r state variables of the original higher-order model. The remaining state variables are given in terms of the first r state variables by Eqn. (105).

E. Robust Decentralized FOS Feedback Technique via Reduced Order Model for the Multimodel System

Let us consider a family of plants $S = \{A_i, B_i, C_i\}$ defined [23] by

$$\dot{x} = A_i x + B_i u,\ \ y = C_i x,\ \ \ i = 1, 2, ..., M. \tag{106}$$

The discrete time invariant systems with sampling interval τ seconds can be represented as

$$x(k+1) = \Phi_{\tau i} x(k) + \Gamma_{\tau i} u(k),\ \ y(k) = C_i x(k). \tag{107}$$

There exists a transformation V_i, such that,

$$x = V_i z \tag{108}$$

transforms the above system in Eqn. (107) into the following block diagonal modal form as

$$z(k+1) = \hat{\Phi}_i z(k) + \hat{\Gamma}_i u(k),\ \ y(k) = \hat{C}_i z(k), \tag{109}$$

where

$$\hat{\Phi}_i = \begin{bmatrix} \Phi_{1i} & 0 \\ 0 & \Phi_{2i} \end{bmatrix}, \hat{\Gamma}_i = \begin{bmatrix} \Gamma_{1i} \\ \Gamma_{2i} \end{bmatrix}, \hat{C}_i = \begin{bmatrix} C_{1i} & C_{2i} \end{bmatrix} \quad (110)$$

and the eigen values are arranged in the order of their dominance. We now extract an r^{th} order model, retaining the r dominant eigen values, by truncating the above systems. Using Eqns. (109) and (110), we get

$$z_r(k+1) = \Phi_{1i}\, z_r(k) + \Gamma_{1i}\, u(k),\ \ y(k) = C_{1i}\, z_r(k) \quad (111)$$

Let $u(k) = S_r\, z_r$ be a stabilizing control for the reduced order model in Eqn. (111). Thus, the closed loop reduced model $\left(\Phi_{1i} + \Gamma_{1i}\, S_r\right)$ becomes stable. Now,

$$Z_r = \left[I_r : 0_{r*(n-r)}\right]\ \ z = \left[I_r : 0_{r*(n-r)}\right] V^{-1} x\,, \quad (112)$$

$\therefore$, we get,

$$u(k) = S_r \left[I_r : 0_{r*(n-r)}\right] V^{-1} x = S_i\, x\,, \quad (113)$$

which makes the closed loop system $\left(\Phi_{\tau i} + \Gamma_{\tau i}\, S_i\right)$ stable and has no eigenvalues at the origin. Thus, $S_i \equiv F_i$ are the stabilizing state feedback gains for the system in Eqn. (107). Using these state feedback gains F_i, the following inequalities are solved.

$$\begin{aligned} &\left\| \mathbf{L} \right\| < \rho_{1i}\,, \\ &\left\| \mathbf{L}\mathbf{D}_{0i} - F_i\, \Gamma_{\tau i} \right\| < \rho_{2i}\,, \\ &\left\| \mathbf{L}\mathbf{C}_i - F_i \right\| < \rho_{3i}\,,\ i = 1, ..., M. \end{aligned} \quad (114)$$

The controller obtained from the above equation will give desired behaviour, but might require excessive control action. To reduce this effect, we relax the condition that $\mathbf{L}$ exactly satisfy the above linear equation and include a constraint on the gain $\mathbf{L}$. Thus, we arrive at the following in equations,

$$\begin{aligned} &\begin{bmatrix} -\rho_{1i}{}^2 I & \mathbf{L} \\ \mathbf{L}^T & -I \end{bmatrix} < 0\,, \\ &\begin{bmatrix} -\rho_{2i}{}^2 I & \mathbf{L}\mathbf{D}_{0i} - F_i\, \Gamma_{\tau i} \\ \left(\mathbf{L}\mathbf{D}_{0i} - F_i\, \Gamma_{\tau i}\right)^T & -I \end{bmatrix} < 0\,, \\ &\begin{bmatrix} -\rho_{3i}{}^2 I & \mathbf{L}\mathbf{C}_i - F_i \\ \left(\mathbf{L}\mathbf{C}_i - F_i\right)^T & -I \end{bmatrix} < 0\,. \end{aligned} \quad (115)$$

If the LMI constraints given in Eqns. (114) and (115) are solved using the above F_i, the robust FOS feedback gain may become full. This results in the control input of each model being a function of the outputs of all the models. To obtain the RDFOS feedback control, the off-diagonal elements of $L_0, L_1, ..., L_{N-1}$ matrices are made equal to zero as a result of which the control input to each actuator is a function of the output of that corresponding sensor only. This makes the FOS control technique a robust decentralized one.

IV. Control Simulations of the Smart Beam

The FEM and the state space model of the smart cantilever beam is developed in MATLAB using Euler-Bernoulli beam theory. The flexible cantilever beam is divided into 4 finite elements and the sensor and actuator as collocated pairs at finite element positions 2 and 4 respectively, thus giving rise to a multivariable beam with 2 inputs and 2 outputs. By varying the thickness of the beam from 0.5, 0.6, 0.7, 0.8 and 1 mm, 5 multivariable models are obtained. A 12^{th} order state space model of the system is obtained on retaining the first 6 modes of vibration of the system. Simulations are carried out in MATLAB. The FOS control technique discussed above is used to design a controller to suppress the 1^{st} 6 vibration modes of a cantilever beam through smart structure concept for the various multivariable models of the smart beam. RDFOS feedback based reduced model order controllers are designed for multimodel smart structure system using the developed multivariable state space model and its performance is evaluated for the Active Vibration Control.

The first task in designing the FOS controller is the selection of the sampling interval τ. The maximum bandwidth for all the sensor / actuator locations on the beam are calculated (here, the 6^{th} vibratory mode of the plant) and then by using existing empirical rules for selecting the sampling interval based on bandwidth, approximately 10 times of the maximum 6^{th} vibration mode frequency of the system has been selected. The sampling interval used is $\tau = 0.004$ seconds. The number of sub-intervals N is chosen to be 10.

An external force f_{ext} of 1 Newton is applied for duration of 50 ms at the free end of the beam for all the 5 models of the Fig. 2. RDFOS Controllers via the reduced order modeling has been designed to control the first 6 modes of vibration of the smart cantilever beam for the 5 models of the smart structure. A large 12^{th} order system of (12×12) is reduced to a simpler 6^{th} order model of (6×6), by considering the effects of the 6 most dominant (dominant in the sense of being closed to instability) eigen values. The eigen values of the original system that are farthest from the origin are neglected and only dominant eigen values of the original system in the reduced order model is retained. The open loop and closed loop responses of the system with the state feedback gain F are observed.

The fast output sampling feedback gain matrix $\mathbf{L}$ for the system given is obtained by solving $\mathbf{L}\mathbf{C} \cong F$ using the LMI optimization method [11] which reduces the amplitude of the control signal u. For convenience, only the closed loop impulse responses (sensor outputs y_1 and y_2) with FOS feedback gain $\mathbf{L}$ of the system and the variation of the control signal u_1 and u_2 with time for the multivariable-multimodel system are shown in Figs. 4 - 13 respectively.

The 5 multivariable models of the smart structure system are considered for designing the RDFOS feedback controller

via the reduced order model using the LMI technique approach of MATLAB. The discrete models are obtained for sampling time of $\tau = 0.004$ seconds. The reduced order models are computed from the adjoint discrete models. Using the method discussed in section III, common stabilizing gain matrix S_r is obtained for the reduced order model using the LMI toolbox. Using aggregation techniques [20], the state feedback gain F_i can be calculated for the higher order (actual model).

This FOS feedback gain can be obtained which approximately realizes the designed F_i for all the models of the family. Here, as we are dealing with robust stabilization, we have to find a $\mathbf{L}$ which will satisfy $\mathbf{L}\mathbf{C}_i = F_i$, $(i = 1 \text{ to } 5)$ all these equations using the LMI approach. The gain sequences of $\mathbf{L}$ are chosen 10 $(L_1, L_2, ..., L_{10})$. Using the F_i, LMI constraints given in Eqns. (114) and (115) are solved for different values of ρ_1, ρ_2 and ρ_3 to find the robust decentralized gain matrix $\mathbf{L}$ via the reduced order model which is given as

$$\mathbf{L} = \begin{bmatrix} 172.1137 & 0 & -79.0428 & 0 \\ 0 & -144.1840 & 0 & 108.1592 \\ -176.0630 & 0 & -68.3585 & 0 \\ 0 & 92.7216 & 0 & 2.2531 \\ 169.2613 & 0 & -9.8467e-006 & \\ 0 & -86.7592 & 0 & \\ 0 & 0.0016 & 0 & -0.0968 \\ 1.2890e-005 & 0 & -0.0020 & 0 \\ 0 & 2.6812 & 0 & -34.4828 \quad 0 \\ 0.1069 & 0 & -2.6288 & 0 \quad 30.4253 \end{bmatrix}_{(2\times 20)} \quad (116)$$

The closed loop responses with this RDFOS feedback gain $\mathbf{L}$ via the reduced order model for all the models are satisfactory and are able to stabilize the outputs. The eigen values of $\left(\Phi^N + \Gamma \mathbf{L} C\right)$ are found to be within the unit circle. It is found that the designed robust decentralized FOS feedback controllers via the reduced order model provide good damping enhancement for the various multivariable models of the smart structure plant. The proposed robust decentralized control for the multimodel smart structure system can be applied simultaneously to all the models and results in satisfactory response behaviour to damp out the vibrations, which can be seen form the simulation results in section 4. The input applied to each actuator of the model is a function of the output of that respective sensor only, which makes the control technique a robust, decentralized one.

V. Conclusion

Robust Decentralized Fast Output Sampling Feedback Controller is designed for the multivariable smart structure using the various models of the single plant via the reduced order modeling. Simulations are done in Matlab and the various responses are obtained for the designed state space based FE model of the smart flexible cantilever beam. Through the simulation results, it is shown that when the plant is placed with the designed robust decentralized FOS controller, the 5 models performs well. In the designed control law, the control input to each actuator of the multivariable plant's multimodel is a function of the output of that corresponding sensor only and the gain matrix has got all off-diagonal elements zero or very small compared to the diagonal terms. This makes the FOS control technique a robust decentralized one. This would render better control.

The robust decentralized FOS controller designed by the above method requires only constant gains and hence is easier to implement. Closed loop responses are simulated for the various multivariable models of the smart structure plant. A new algorithm is presented for the design of robust decentralized controllers for a multivariable system using FOS feedback technique via the reduced order model. The computation of the state feedback gain, which is needed to obtain the decentralized FOS feedback based smart structure system, becomes very tedious when a number of modes, especially greater than 5 are considered.

Here, a state feedback gain is computed from the reduced order model of the smart system and using the aggregation techniques, a state feedback gain can be obtained for the higher order (actual model). The RDFOS feedback gain which realizes this state feedback gain, can be obtained for the actual model. It is found that the designed and proposed robust controller via the reduced order model provides good damping enhancement for the models of the smart structure system. Thus, an integrated finite element model to analyze the vibration suppression capability of a smart cantilever beams with surface mounted piezoelectric devices based on Euler-Bernoulli beam theory and reduced order modeling is presented in this paper.

VI. Simulation Results

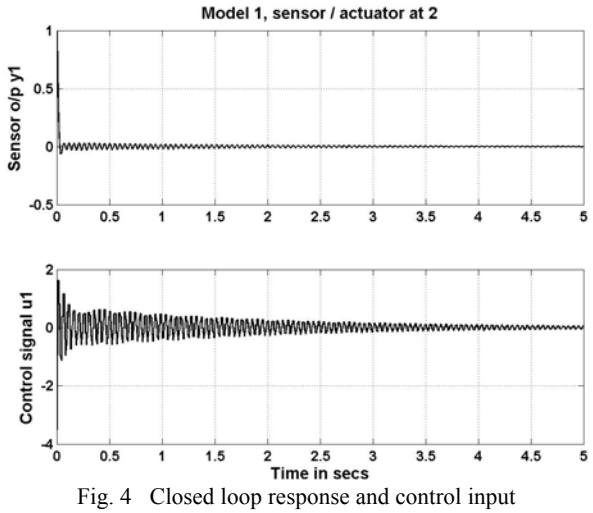

Fig. 4 Closed loop response and control input (sensor / actuator placed at FE 2) : Model 1

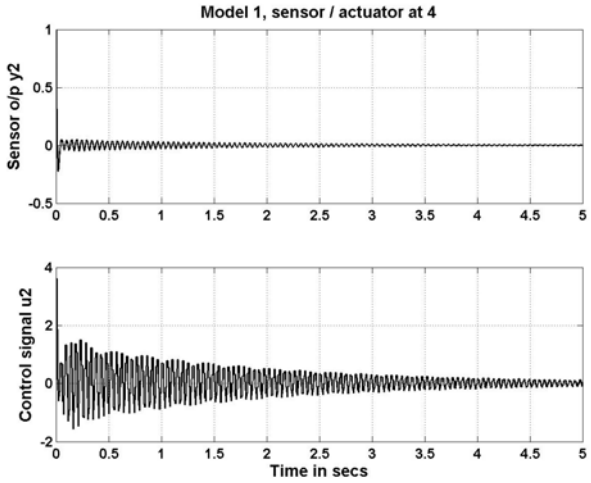

Fig. 5 Closed loop response and control input (sensor / actuator placed at FE 4) : Model 1

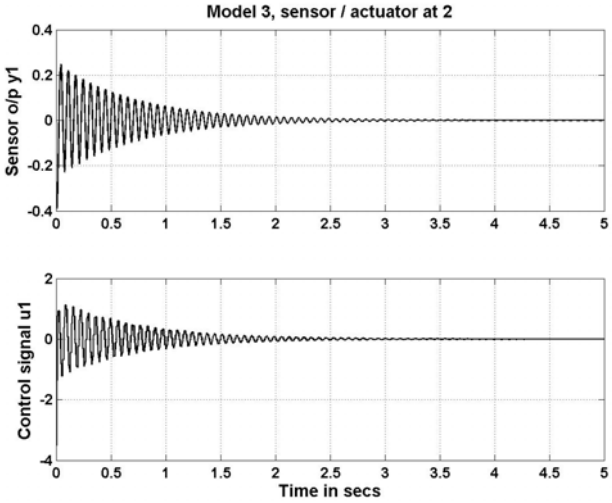

Fig. 6 Closed loop response and control input (sensor / actuator placed at FE 2) : Model 2

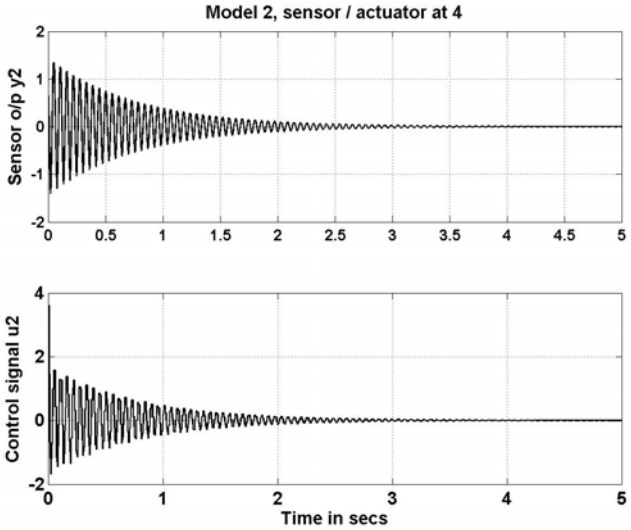

Fig. 7 Closed loop response and control input (sensor / actuator placed at FE 4) : Model 2

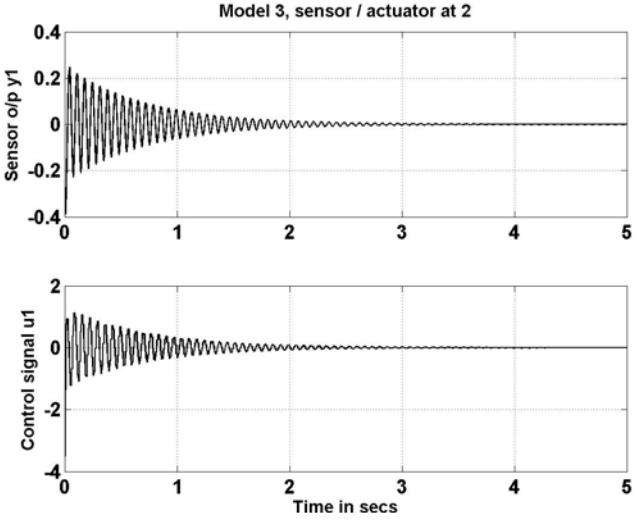

Fig. 8 Closed loop response and control input (sensor / actuator placed at FE 2) : Model 3

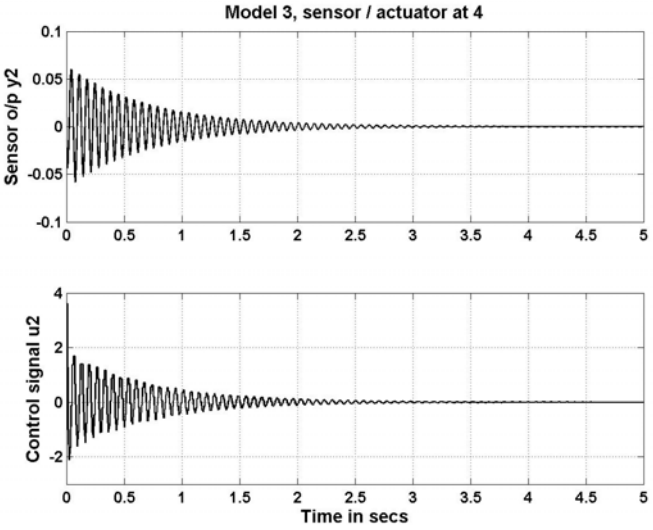

Fig. 9 Closed loop response and control input (sensor / actuator placed at FE 4) : Model 3

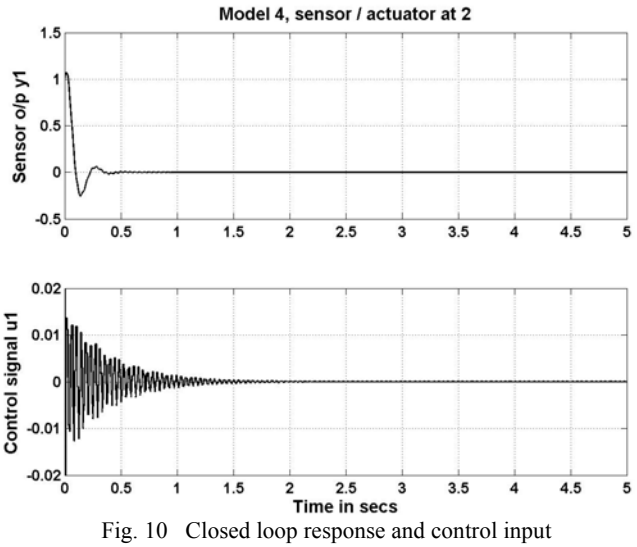

Fig. 10 Closed loop response and control input (sensor / actuator placed at FE 2) : Model 4

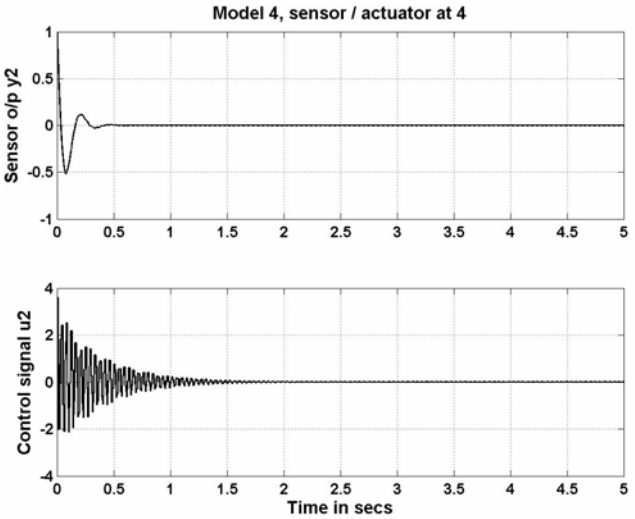

Fig. 11 Closed loop response and control input (sensor / actuator placed at FE 4) : Model 4

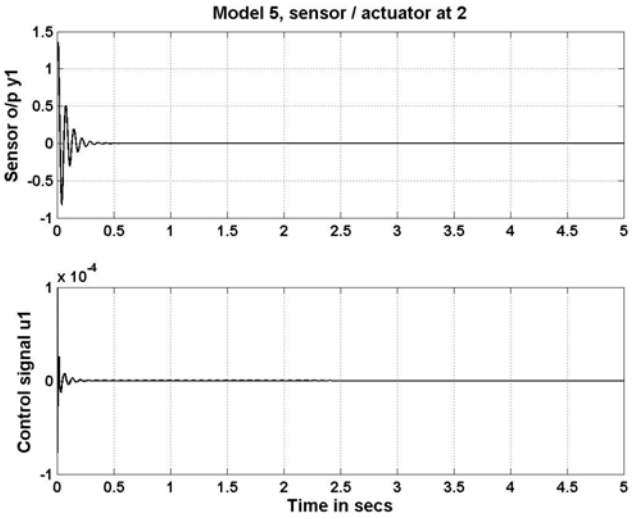

Fig. 12 Closed loop response and control input (sensor / actuator placed at FE 2) : Model 5

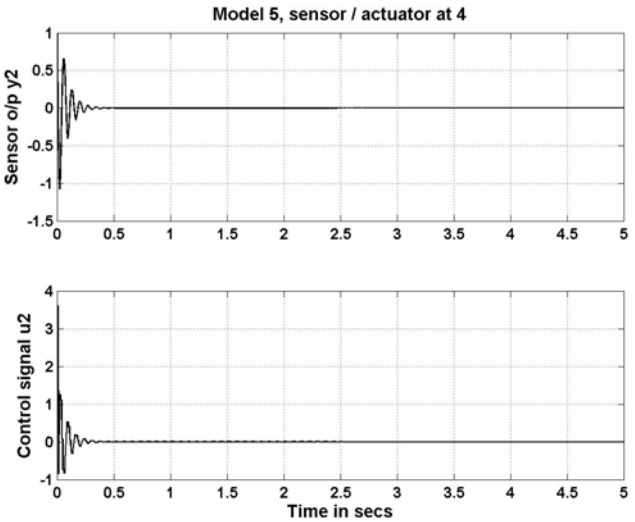

Fig. 13 Closed loop response and control input (sensor / actuator placed at FE 4) : Model 5

ACRONYMS / ABBREVIATIONS

SISO	Single Input Single Output
FEM	Finite Element Method
FE	Finite Element
LMI	Linear Matrix Inequalities
MR	Magneto Rheological
ER	Electro Rheological
PVDF	Poly Vinylidene Fluoride
SMA	Shape Memory Alloys
CF	Clamped Free
CC	Clamped Clamped
CT	Continuous Time
DT	Discrete Time
OL	Open Loop
CL	Closed Loop
HOBT	Higher Order Beam Theory
RHS	Right Hand Side
LTI	Linear Time Invariant
FOS	Fast Output Sampling
AVC	Active Vibration Control
EB	Euler-Bernoulli
PZT	Lead Zirconate Titanate
DOF	Degree Of Freedom
IEEE	Institute of Electrical & Electronics Engineers
IOP	Institute of Physics
ISSS	Institute of Smart Structures and Systems
SPIE	Society of Photonics & Instrumentation Engineers

APPENDIX

The stiffness matrix for the sandwich beam element is obtained using the Eqn. (65) as

$$[K]=\begin{bmatrix} K_{11} & K_{12} & K_{13} & K_{14} & K_{15} & K_{16} \\ K_{21} & K_{22} & K_{23} & K_{24} & K_{25} & K_{26} \\ K_{31} & K_{32} & K_{33} & K_{34} & K_{35} & K_{36} \\ K_{41} & K_{42} & K_{43} & K_{44} & K_{45} & K_{46} \\ K_{51} & K_{52} & K_{53} & K_{54} & K_{55} & K_{56} \\ K_{61} & K_{62} & K_{63} & K_{64} & K_{65} & K_{66} \end{bmatrix},$$

where

$$K_{11}=\frac{A\,A_{11}}{L},\ K_{12}=K_{21}=\frac{A\,B_{11}}{L},\ K_{13}=K_{31}=0$$

$$K_{14}=K_{41}=-\frac{A\,A_{11}}{L},\ K_{15}=K_{51}=-\frac{A\,B_{11}}{L}$$

$$K_{16}=K_{61}=0,\ K_{24}=K_{42}=-\frac{A\,B_{11}}{L}$$

$$K_{34}=K_{43}=0$$

$$K_{22}=-\frac{1}{10}\frac{AL\{D_{11}L^3-10B_{11}\gamma L^2+60A_{55}L+60\eta^2 A_{11}L+120\gamma B_{11}\eta\}}{\left(12\eta-L^2\right)^2}$$

$$K_{23} = K_{32} = \frac{6}{5}\frac{A}{L}\frac{[D_{11}L^4 + 10A_{55}L^2 + 10\gamma^2 L^2 A_{11} - 20L^2 D_{11}\eta + 120 D_{11}\eta^2]}{(12\eta - L^2)^2}$$

$$K_{25} = K_{52} = -\frac{6}{5}\frac{A}{L}\frac{[D_{11}L^4 + 10A_{55}L^2 + 10\gamma^2 L^2 A_{11} - 20L^2 D_{11}\eta + 120 D_{11}\eta^2]}{(12\eta - L^2)^2}$$

$$K_{26} = K_{62} = \frac{1}{10}\frac{AL[-D_{11}L^3 - 10B_{11}\gamma L^2 - 60A_{55}L - 60\gamma^2 A_{11}L + 120\gamma B_{11}\eta]}{(12\eta - L^2)^2}$$

$$K_{33} = \frac{\{A(2L^6 D_{11} - 30L^4 D_{11}\eta + 180L^2 D_{11}\eta^2 - 15L^5\gamma B_{11} + 2160A_{55}\eta^2 + 60A_{55}L^4 - 360A_{55}\eta L^2 + 180\gamma L^3 B_{11}\eta + 45\gamma^2 L^4 A_{11})\}}{15L(12\eta - L^2)^2}$$

$$K_{35} = K_{53} = \frac{1}{10}\frac{AL\{D_{11}L^3 - 10B_{11}\gamma L^2 + 60A_{55}L + 60\gamma^2 A_{11}L + 120\gamma B_{11}\eta\}}{(12\eta - L^2)^2}$$

$$K_{36} = K_{63} = \frac{-A[L^6 D_{11} - 60A_{55}L^4 - 90\gamma^2 L^4 A_{11} - 60L^4 D_{11}\eta + 360L^2 D_{11}\eta^2 + 4320A_{55}\eta^2 - 720A_{55}\eta L^2]}{30L(12\eta - L^2)^2}$$

$$K_{44} = \frac{AA_{11}}{L}$$

$$K_{45} = K_{54} = \frac{AB_{11}}{L}$$

$$K_{46} = K_{64} = 0$$

$$K_{55} = \frac{6}{5}\frac{A}{L}\frac{\{D_{11}L^4 + 10A_{55}L^2 + 10\gamma^2 L^2 A_{11} - 20L^2 D_{11}\eta + 120 D_{11}\eta^2\}}{(12\eta - L^2)^2}$$

$$K_{56} = K_{65} = -\frac{1}{10}\frac{AL\{-D_{11}L^3 - 10B_{11}\gamma L^2 - 60A_{55}L - 60\gamma^2 A_{11}L + 120\gamma B_{11}\eta\}}{(12\eta - L^2)^2}$$

$$K_{66} = \frac{\{A(2L^6 D_{11} + 15L^5\gamma B_{11} - 30L^4 D_{11}\eta + 60A_{55}L^4 + 45\gamma^2 L^4 A_{11} - 180\gamma L^3 B_{11}\eta + 180L^2 D_{11}\eta^2 - 360A_{55}\eta L^2 + 2160A_{55}\eta^2)\}}{15L(12\eta - L^2)^2}$$

The mass matrix for the sandwich beam element is obtained using Eqn. (61) as

$$[M] = \begin{bmatrix} M_{11} & M_{12} & M_{13} & M_{14} & M_{15} & M_{16} \\ M_{21} & M_{22} & M_{23} & M_{24} & M_{25} & M_{26} \\ M_{31} & M_{32} & M_{33} & M_{34} & M_{35} & M_{36} \\ M_{41} & M_{42} & M_{43} & M_{44} & M_{45} & M_{46} \\ M_{51} & M_{52} & M_{53} & M_{54} & M_{55} & M_{56} \\ M_{61} & M_{62} & M_{63} & M_{64} & M_{65} & M_{66} \end{bmatrix},$$

where

$$M_{11} = \frac{1}{3}LI_1,\quad M_{12} = M_{21} = \frac{1}{2}\frac{\gamma L^2 I_1}{(12\eta - L^2)}$$

$$M_{13} = M_{31} = -\frac{1}{4}\frac{\gamma L^3 I_1}{(12\eta - L^2)}$$

$$M_{14} = M_{41} = \frac{1}{6}LI_1$$

$$M_{15} = M_{51} = -\frac{1}{2}\frac{\gamma L^2 I_1}{(12\eta - L^2)}$$

$$M_{16} = M_{61} = -\frac{1}{4}\frac{\gamma L^3 I_1}{(12\eta - L^2)}$$

$$M_{22} = \frac{1}{35}\frac{L[-294I_3\eta L^2 + 35I_2 L^3 + 1680I_3\eta^2 + 13I_3 L^4 - 420I_2\eta L + 42I_1 L^2 + 42\gamma^2 I_1 L^2]}{(12\eta - L^2)^2}$$

$$M_{23} = M_{32} = \frac{\{-L(11I_3 L^5 - 10080I_2\eta^2 + 1260I_3\eta^2 L - 231I_3 L^3\eta + 126\gamma^2 I_1 L^3 + 1260LI_1\eta + 840I_2\eta L^2 + 21I_1 L^3)\}}{210(12\eta - L^2)^2}$$

$$M_{24} = M_{42} = \frac{1}{2}\frac{\gamma L^2 I_1}{(12\eta - L^2)}$$

$$M_{25} = M_{52} = \frac{3}{70}\frac{L[3I_3 L^4 - 28\gamma^2 I_1 L^2 - 28I_1 L^2 - 84I_3\eta L^2 + 560I_3\eta^2]}{(12\eta - L^2)^2}$$

$$M_{26} = M_{62} = \frac{[L(13I_3 L^5 + 10080I_2\eta^2 + 2520I_3\eta^2 L - 378I_3 L^3\eta - 252\gamma^2 I_1 L^3 - 2520LI_1\eta - 840I_2\eta L^2 - 42I_1 L^3)]}{420(12\eta - L^2)^2}$$

$$M_{33} = \frac{[L(252I_3\eta^2 L^2 - 42I_3 L^4\eta + 63\gamma^2 I_1 L^4 - 420I_1\eta L^2 - 2520I_2\eta^2 L + 210I_2\eta L^3 + 10080I_1\eta^2 + 28I_1 L^4 + 2I_1 L^6)]}{210(12\eta - L^2)^2}$$

$$M_{34} = M_{43} = -\frac{1}{4}\frac{\gamma L^3 I_1}{(12\eta - L^2)}$$

$$M_{35} = M_{53} = \frac{[L(13I_3 L^5 - 10080I_2\eta^2 + 2520I_3\eta^2 L - 378I_3 L^3\eta - 252\gamma^2 I_1 L^3 - 2520LI_1\eta + 840I_2\eta L^2 - 42I_1 L^3)]}{420(12\eta - L^2)^2}$$

$$M_{36} = M_{63} = \frac{[-L(504I_3\eta^2 L^2 - 84I_3 L^4\eta - 126\gamma^2 I_1 L^4 - 840I_1\eta L^2 - 10080I_1\eta^2 + 14I_1 L^4 + 3I_3 L^6)]}{420(12\eta - L^2)^2}$$

$$M_{44} = \frac{1}{3} L I_1,\ M_{45} = M_{54} = -\frac{1}{2} \frac{\gamma L^2 I_1}{\left(12\eta - L^2\right)}$$

$$M_{46} = M_{64} = -\frac{1}{4} \frac{\gamma L^3 I_1}{\left(12\eta - L^2\right)}$$

$$M_{55} = \frac{1}{35} \frac{\begin{array}{l}[L(13 I_3 L^4 - 35 I_2 L^3 + 42\gamma^2 I_1 L^2 \\ + 42 I_1 L^2 - 294 I_3 \eta L^2 + 420 I_2 \eta L \\ + 1680 I_3 \eta^2)]\end{array}}{\left(12\eta - L^2\right)^2}$$

$$M_{56} = M_{65} = \frac{\begin{array}{l}[L\ (11 I_3 L^5 - 231 I_3 L^3 \eta + 126\gamma^2 I_1 L^3 - \\ 840 I_2 \eta L^2 + 21 I_1 L^3 + 1260 L I_1 \eta \\ + 1260 I_3 \eta^2 L + 10080 I_2 \eta^2)]\end{array}}{210\left(12\eta - L^2\right)^2}$$

$$M_{66} = \frac{\begin{array}{l}[L\ (252 I_3 \eta^2 L^2 - 42 I_3 L^4 \eta + 63\gamma^2 I_1 L^4 \\ - 420 I_1 \eta L^2 + 2520 I_2\ \eta^2 L - 210 I_2 \eta L^3 \\ + 10080 I_1 \eta^2 + 28 I_1 L^4 + 2 I_3 L^6)]\end{array}}{210\left(12\eta - L^2\right)^2}$$

NOMENCLATURE (LIST OF SYMBOLS)

A	Area of the piezo patches
a_1, a_2, a_3, a_4	Polynomial coefficients for transverse displacement
$\mathbf{A}$	System matrix which represents dynamics of system (comprises of mass and stiffness of system)
A_{11}, A_{55}	Extensional and shear stiffness coefficient
B_{11}	Bending-extensional stiffness coefficient
$\mathbf{B}$	Input matrix
b_1, b_2, b_3	Polynomial coefficients for
c	Width of the beam
c_1, c_2, c_3	Polynomial coefficients for axial displacement
$\mathbf{C}$	Output matrix
$\mathbf{C}^*$	Generalized damping matrix or the structural modal damping matrix
$\mathbf{C}_0$	Fictitious matrix
$\mathbf{D}$	Transmission matrix
$\mathbf{D}_0$	Fictitious matrix
D_{11}	Bending stiffness coefficient
D	Layer constitutive matrix
D_3	Electric displacement in the thickness direction
d_{15}, d_{31}	Piezoelectric strain constants
E_{11}	Actuator induced axial force
e_{15}	Piezoelectric constant
E_f	Electric potential applied to the actuator
$\mathbf{E}$	External load matrix, which couples the disturbance to the system
$\mathbf{f}_{ext}$	Vector of externally applied nodal forces
f^t	Total force vector
$\mathbf{f}_{ctrl}$	Control force vector
$\mathbf{f}^*_{ext}, \mathbf{f}^*_{ctrl}$	Generalized external force coefficient and external control force coefficient vector
$\mathbf{f}^*_{ctrl\,1}, \mathbf{f}^*_{ctrl\,2}$	Control force coefficient vectors to the actuators 1 and 2
F_{11}	Actuator induced bending moment
F	State feedback gain
F_1 and F_2	Forces at node 1 and 2 of figure 1
G_{55}	Actuator induced shear force
G_c	Signal conditioning gain
G	Modulus of rigidity
$\mathbf{g}$	Principal coordinates
$\bar{h}$	Height of the beam + the piezo-patches
$\mathbf{h}$	Constant vector, which depends on the type of actuator and its FE position
$\mathbf{h}_1, \mathbf{h}_2$	Constant vectors of the actuators 1 and 2
I_1, I_2, I_3	Mass inertias
I	Inertia matrix
i	Variable (1, 2, 3, …)
$i(t)$	Current induced by the sensor surface
$\mathbf{K}, \mathbf{K}^*$	Stiffness matrix (global stiffness matrix) and generalized stiffness matrix of the beam
k	Variable (1, 2, 3, …)
K_c	Gain of the controller
K	Shear correction factor = 5/6
K_{ij}	Elements of the stiffness matrix $(i, j = 1, 2, ..., 6)$ for the sandwich / composite beam
$\mathbf{L}$	Fast output sampling feedback gain
L	Length of the beam
L_p	Length of the piezo-patch (sensor / actuator)
L_j	Output feedback gains
$\mathbf{M}, \mathbf{M}^*$	Mass matrix (global mass matrix) and generalized mass matrix of the beam
M_{ij}	Elements of the mass matrix $(i, j = 1, 2, ..., 6)$ for the sandwich / composite beam
M_1 and M_2	Moments acting at node 1 and 2 of figure 1

M_x	Internal force on the cross section of the beam
N_u, N_w, N_θ	Shape functions due to axial displacement, transverse displacement and rotation or the slope
$N_1,...., N_6$	Elements of shape function due to axial displacement
$N_7,...., N_{10}$	Elements of shape function due to transverse displacement
$N_{11},...., N_{14}$	Elements of shape function due to rotation or slope
n	Number of layers of the beam
N	Number of sub-intervals
N	Matrix of shape functions
N_x	Internal force on the cross section of the beam
$\mathbf{p}$	Constant vector, which depends on the sensor type and its FE location in the embedded structure
$\mathbf{p}_1, \mathbf{p}_2$	Constant vectors of the sensors 1 and 2
$q(t)$	Charge accumulated on the sensor surface
$\dot{q}(t)$	Rate of change of electric charge, i.e., the current produced by sensor
$\mathbf{q}$	Vector of nodal displacements (modal coordinate vector), i.e., the generalized coordinates
q_0	Transverse distributed loading
$r(t)$	External force input to the beam
$\dot{\mathbf{q}}$	Time derivative of the nodal coordinate vector
$\ddot{\mathbf{q}}$	Nodal acceleration vector
$Q_{11}, Q_{12}, Q_{13}, Q_{22}, Q_{55}, Q_{66}$	Material constants of steel, foam, PE
Q_{xz}	Internal force on the cross section of the beam
$\mathbf{T}$	Modal matrix containing the eigen values representing the first 3 modes of vibration
t	Time
T	Kinetic energy
t	Total thickness of the beam (top layer + piezo-patch + bottom layer thickness)
t_k	Thickness of the each layer of the beam $k = 1,2,3$
t_p	Thickness of the piezoelectric layer
$t_a = t_s = t_p$	Thickness of actuator / sensor = thickness of the piezoelectric layer
u	Axial displacement of the point
u_1, u_2	Axial displacements at fixed end and at free end
$u_1(t), u_2(t)$	Control inputs to actuators 1 and 2
U	Strain energy
$\mathbf{V}^a, \mathbf{V}^s$	Actuator input voltage and sensor voltage

REFERENCES

[1] Baily, T. and Hubbard Jr., J.E., "Distributed Piezoelectric Polymer Active Vibration Control of A Cantilever Beam", *J. of Guidance, Control and Dynamics*, Vol. 8, no. 5, pp. 605 – 611, 1985.

[2] Crawley, E.F. and De Luis, J., "Use of Piezoelectric Actuators as Elements of Intelligent Structures", *AIAA J.*, Vol. 25, pp. 1373–1385, 1987.

[3] Culshaw, B., "Smart Structures - A Concept or A Reality," *J. of Systems and Control Engg.*, Vol. 26, no. 206, pp. 1– 8, 1992.

[4] Choi, S.B., Cheong, C. and S. Kini. (1995), "Control of Flexible Structures by Distributed Piezo-film Actuators and Sensors", *J. of Intelligent Materials and Structures*, 16, 430 - 435.

[5] Fanson, J. L. and Caughey, T.K., "Positive Position Feedback Control For Structures," *AIAA J.*, Vol. 18, no. 4, 717–723, 1990.

[6] Hanagud, S., Obal, M.W. and Callise, A.J., "Optimal Vibration Control By The Use of Piezoceramic Sensors and Actuators", *J. of Guidance, Control and Dynamics*, Vol. 15, no. 5, pp. 1199 – 1206, 1992.

[7] Hwang, W. and Park H.C., "Finite Element Modeling of Piezoelectric Sensors and Actuators", *AIAA J.*, Vol. 31, no. 5, pp. 930 – 937, 1993.

[8] Syrmos, V.L., Abdallah, P., Dorato, P. and Grigoriadis, K., "Static Output Feedback A Survey", *Automatica*, Vol. 33, no. 2, pp.125 –137, 1997.

[9] Werner, H. and Furuta, K., "Simultaneous Stabilization Based on Output Measurements", *Kybernetika*, Vol. 31, no. 4, pp. 395 – 411, 1995.

[10] Werner, H., "Multimodal Robust Control by Fast Output Sampling - An LMI Approach," *Automatica*, Vol. 34, no. 12, pp. 1625 – 1630, 1998.

[11] Yong-Yan Cao, Lam, J. and Sun, Y.X. "Static Output Feedback Stabilization: An LMI Approach", *Automatica*, Vol. 34, no. 12, pp. 1641-1645, 1998.

[12] Rao, S. and M. Sunar, "Piezoelectricity and its uses in disturbance sensing and control of flexible structures : A survey," *Applied Mechanics Rev.* Vol. 47, no. 2, pp. 113 – 119, 1994.

[13] Mark Balas, J., "Feedback Control of Flexible Structures," *IEEE Trans. Automat. Contr.*, Vol. AC-23, no. 4, pp. 673-679, 1978.

[14] Herbert Werner and Tile Meister, "Robust Control of a Laboratory Aircraft Model Via Fast Output Sampling," *Control Engineering Practice*, Vol. 7, pp. 305-313, 1999.

[15] Hwang Woo Seok and Hyun Chul Park, "Finite element modeling of piezo-electric sensors and actuators," *IEEE Trans. Automat. Contr.* Vol. 31, no. 5, pp. 930 – 937, 1993.

[16] Chammas, A. B. and C. T. Leondes, "Pole placement by piecewise constant output feedback," *Int. J. Contr.*, Vol. 29, no. 1, pp. 31-38, 1979.

[17] Davison, E.J., "A method for simplifying linear dynamical systems," *IEEE Trans. Auto. Contr.*, Vol. AC-11, pp. 93-101, 1966.

[18] Lamba, S.S. and Rao, S.V., "On the suboptimal control via the simplified model of Davison," *IEEE Trans. Auto. Contr.*, Vol. AC-19, pp. 448-450, 1974.

[19] Mahmoud, M.S. and G.M. Singh, "Large scale systems modeling," *Pergamon Press*, Oxford, 1981.

[20] Aoki, M., "Control of large scale dynamic systems by aggregation," *IEEE Trans. Auto. Contr.*, Vol. AC-13, no. 3, 246-253, 1968.

[21] Manjunath, T.C., and B. Bandyopadhyay., "Controller Design for Euler-Bernoulli Smart Structures Using Robust Decentralized POF via Reduced Order Modeling", Vol. 3, no.3, pp. 205-221, 2006.

[22] Umapathy, M., and B. Bandyopadhyay, "Control of flexible beam through smart structure concept using periodic output feedback," *System Science Journal*, vol. 26, no. 1, pp. 23 - 46, 2000.

[23] Rajeev, G., Bandyopadhyay, B., and Kulkarni A.M., "Robust decentralized periodic output feedback technique based power system stabilizer for multi machine power system", *IEE Proc., Control Theory Appl.*, Vol. 152, pp. 3–8, 2005.

T. C. Manjunath, born in Bangalore, Karnataka, India on Feb. 6, 1967 received the B.E. Degree in Electrical Engineering from the University of Bangalore in 1989 in First Class and M.E. in Electrical Engineering with specialization in Automation, Control and Robotics from the University of Gujarat in 1995 in First Class with Distinction, respectively. He has got a teaching experience of 17 long years in various engineering colleges all over the country and is currently a Research Scholar in the department of systems and control engineering, Indian Institute of Technology Bombay, India in the field of modeling, simulation, control and implementation of smart flexible structures using DSpace and its applications.

B. Bandyopadhyay, born in Birbhum village, West Bengal, India, on 23rd August 1956 received his Bachelor's degree in Electronics and Communication Engineering from the University of Calcutta, Calcutta, India, and Ph.D. in Electrical Engineering from the Indian Institute of Technology, Delhi, India in 1978 and 1986, respectively. In 1987, he joined the Interdisciplinary Programme in Systems and Control Engineering, Indian Institute of Technology Bombay, India, as a faculty member, where he is currently a Professor.